PNNL-13746

Pacific Northwest
National Laboratory
Operated by Battelle for the
U.S. Department of Energy

Feasibility of In Situ Redox Manipulation of Subsurface Sediments for RDX Remediation at Pantex

J. E. Szecsody
J. S. Fruchter
M. A. McKinley
C. T. Resch
T. J. Gilmore

December 2001

Prepared for the U.S. Department of Energy
under Contract DE-AC06-76RL01830

DISCLAIMER

PACIFIC NORTHWEST NATIONAL LABORATORY
operated by
BATTELLE
for the
UNITED STATES DEPARTMENT OF ENERGY
under Contract DE-AC06-76RL01830

Printed in the United States of America

Available to DOE and DOE contractors from the
Office of Scientific and Technical Information,
P.O. Box 62, Oak Ridge, TN 37831-0062;
ph: (865) 576-8401
fax: (865) 576-5728
email: reports@adonis.osti.gov

Available to the public from the National Technical Information Service,
U.S. Department of Commerce, 5285 Port Royal Rd., Springfield, VA 22161
ph: (800) 553-6847
fax: (703) 605-6900
email: orders@ntis.fedworld.gov
online ordering: http://www.ntis.gov/ordering.htm


This document was printed on recycled paper.
(8/00)

PNNL-13746

Feasibility of In Situ Redox Manipulation of Subsurface Sediments for RDX Remediation at Pantex

J. E. Szecsody
J. S. Fruchter
M. A. McKinley
C. T. Resch
T. J Gilmore

December 2001

Prepared for
the U.S. Department of Energy
under Contract DE-AC06-76RL01830

Pacific Northwest National Laboratory
Richland, Washington 99352

Abstract

This laboratory study was conducted to assess RDX (hexahydro-1,3,5-trinitro-1,3,5 triazine) abiotic degradation by chemically reduced sediments and other geochemical aspects of the application of this technology to remediation of RDX contamination in groundwater at the U.S. Department of Energy Pantex facility. Laboratory experiments showed that chemical reduction of Pantex aquifer sediments using sodium dithionite yielded a high redox capacity (0.4% Fe^{II}/g), which is higher or equal to that achieved at other sites in which field-scale remediation is in progress or being considered. This mass of reducible iron represents sufficient quantity to remain anoxic for hundreds of pore volumes in the field, so would last dozens of years, depending on aquifer flow rates and oxygen diffusion.

RDX was quickly degraded (i.e., minutes) in batch studies using abiotic, reduced sediments (iron reducing conditions) to at least the fourth degradation product. The initial reduction pathway was the same as the biotic pathway (RDX -> MNX -> DXN -> TNX). Simulation of the sequential RDX degradation pathway generally tracked mass fluxes, but indicated that other processes (e.g., sorption) also influenced rates. The rate and extent of *anaerobic* mineralization in these abiotic systems was slow (2 to 4% in 500 h). There was additional *aerobic* abiotic and biotic mineralization (1 and 5%). Pantex sediments degraded RDX quickly in packed columns, which represents idealized flow conditions in the perched aquifer. Degradation rates (half–life) were 18 min for RDX, <1 min for MNX and DXN, and 10 min for TXN. Slow abiotic mineralization was also observed in columns (half-life 100 h). These degradation rates were maintained for 260 pore volumes, demonstrating that a reduced sediment barrier with only a few hours of reaction time is needed to maintain the degradation observed. Because anaerobic mineralization rates were slow, the most viable field-scale solution may be initial anaerobic, abiotic degradation of RDX (i.e., reduced sediment barrier) followed by aerobic biotic mineralization, which was observed to be tenfold faster.

In summary, the use of a chemical reductant to reduce iron oxide phases in sediments shows great promise for application to the Pantex perched aquifer. Final applicability depends not only on these geochemical considerations, but additionally on hydrogeologic and injection design considerations to achieve a viable and economic remediation in the deep (260-ft [80 m]) aquifer.

Acknowledgments

The authors wish to acknowledge the U.S. Department of Energy Innovative Technology and Remediation Demonstration (ITRD) for funding this study and thank Dr. Jim Phelan and other members of the ITRD committee for discussions during this study. The authors would also like to thank Dr. Steve Comfort at University of Nebraska, Lincoln for providing the ^{14}C-RDX and direction for mineralization studies.

Contents

Figures

Table

1.0 Introduction

This report describes results of a laboratory study of RDX (hexahydro-1,3,5-trinitro-1,3,5 triazine) degradation in Pantex sediments. The objectives of this experimental and modeling study were to quantify geochemical and microbial aspects of the applicability of In Situ Redox Manipulation (ISRM) to the RDX-contaminated aquifer at the Pantex site. Specific objectives were to determine if: a) dithionite-reduced sediment degrade RDX, b) dithionite-reduced Pantex sediments can degrade RDX at a rate sufficient to consider remediation, c) the influence of flow in a porous media system on the RDX degradation rate, and d) how long the barrier can be expected to last.

Laboratory experiments used to meet these objectives included: a) sediment reduction and oxidation studies, b) RDX abiotic and biotic degradation studies in batch systems, and c) RDX degradation during transport in 1-D columns. Multiple reaction modeling was used to quantify the reactant mass fluxes and reaction rates. The RDX degradation rate and pathway information was quantified primarily in batch experiments, which provide the most complete pathway information, because data are not influenced by flow. However, complex geochemical rates have been shown to occur at somewhat different rates in columns relative to batch systems, due in part to significantly higher sediment-to-water ratio and slower access to surface sites by mobile constituents. Therefore, RDX degradation pathway rates were also measured in columns, which are more relevant to field-scale rates.

Results of these experiments would need to be used in conjunction with other geochemical and hydraulic characterization at the Pantex facility to design the field-scale injection experiment and predict barrier longevity. For example, the sediment reduction rate influences the injection rate and lag time before extraction in the field experiment because the reduction rate controls the amount of time required for the dithionite solution to fully react with sediments.

2.0 Geochemical Reactions for Remediation of RDX

The in situ geochemical reduction technology being tested on Pantex sediment in this study is based on the presumption that RDX abiotic degradation by zero valent iron (Singh et al. 1998, 1999) is similar to abiotic degradation by reduced (ferrous) iron phases in natural sediments. Previous laboratory studies have shown that dithionite-reduced smectite clays can reduce TNT and RDX[1] within tens of hours. Because the environment created by reducing sediments with dithionite differs from Fe^0 walls (not as reducing; presence of clay and iron oxide catalysts), reaction pathways may differ. In the following sections, the major the reduction and oxidation reactions in sediments are described, then the RDX degradation pathway.

2.1 Iron Reduction Mechanism

The proposed technology uses existing iron in aquifer sediment that is chemically treated with a reductant (sodium dithionite buffered at high pH) for a short time into the contaminated sediment (typically 24 to 60 h) to reduce Fe(III)-oxides present in the sediment to adsorbed or structural Fe(II) phases. This reduction process of aquifer sediments result in the groundwater redox conditions becoming reducing and the disappearance of dissolved oxygen in water.

Reduced iron phases in sediment by this chemical treatment may behave similarly as zero-valent permeable iron walls for some reactions such as trichloroethylene (TCE) dechlorination[2] and chromate reduction (Fruchter et al. 2000). Zero valent iron/mixed metal barriers also rely on the oxidation of ferrous (adsorbed or Fe(II) minerals such as green rust) to ferric iron as the electron donor for remediation of chlorinated aliphatic contaminants (Balko and Tratnyek 1998; Mayer et al. 2000) or reduction of metals such as chromate (Buerge and Hug 1997) and not the oxidation of Fe^0. Although aqueous Fe(II) can reduce chromate (Eary and Rai 1988), adsorbed or structural Fe(II) on an Fe(III)-oxide, clay surface, or zero-valent iron surface is necessary for dechlorination reactions, although the role of the surface is not clearly understood.

The dithionite chemical treatment dissolves and reduces amorphous and some crystalline Fe(III) oxides. The reduced Fe(II) created by the dithionite chemical treatment appears to be present in several different Fe(II) phases: adsorbed Fe(II), Fe(II)-carbonate (siderite), and FeS (iron sulfite), although adsorbed Fe(II) appears to be the dominant Fe(II) phase. There may be other, unidentified Fe(II) mineral phases produced. Although more than one iron (III) phase is likely reduced in a natural sediment, it can

[1] Amonette, J. 2000. "Iron Redox Chemistry of Clays and Oxides: Environmental Applications," book chapter, chapter in A. Fitch (ed.) Electrochemistry of Clays, CMS Workshop Lectures, Clay Minerals Society, Aurora, Colorado, in review.

[2] Szecsody, J., M. Williams, J. Fruchter, and V. Vermeul. 2001. "In Situ Reduction of Aquifer Sediments for Remediation: 1. Iron Reduction Mechanism." Submitted to *Environmental Science and Technology*.

be useful to determine how simple a chemical model is needed to generally describe the observations. The reaction that describes a single phase of iron that is reduced by sodium dithionite:

$$S_2O_4^{-2} + 2{\equiv}Fe^{3+} + 2H_2O \text{ <==> } 2\ddot{y}{\equiv}Fe^{2+} + 2SO_3^{-2} + 4H^+ \quad (1)$$

shows that the forward rate is a function of the dithionite concentration and the square of the reducible iron concentration (rate is overall a third-order function of concentration). The aqueous Fe(II) produced has a high affinity for surfaces, so is quickly adsorbed. Therefore, Fe(II) mobility in mid- to high pH, low ionic strength groundwater is extremely limited, and iron is not expected to leach from sediments during the dithionite treatment. Aqueous iron measurements in previous studies have shown <1% iron leaching even after 600 pore volumes of groundwater through a sediment column. Corresponding solid iron measurements of sediments used in these columns showed 4 to 10% loss of iron. Iron mobility is somewhat higher during the actual dithionite injection, as a high ionic strength solution of other cations (~0.3 mol/L in this case) compete for the same adsorption sites as Fe^{2+}, so cause some Fe^{2+} desorption. Previous experimental transport studies with dithionite injection into sediments have shown 0 to 12% iron loss after 40 pore volumes of dithionite treatment (Szecsody et al. 2000a).

Experimental evidence from previous studies with Hanford sediments has shown that two parallel reduction reactions are needed to describe iron reduction data (i.e., a fraction of sites are quickly reduced and a fraction more slowly reduced). This may be the result of the reduction of two or more major Fe(III) phases. If the number of slowly reducing sites is small, and the mass of iron is far in excess of the dithionite, reaction 1 can be reduced to a first-order reaction in which Fe^{3+} remains constant. Another reaction occurs in the system, which describes the disproportionation of dithionite in contact with sediment:

$$2S_2O_4^{-2} + H_2O \text{ <==> } S_2O_3^{-2} + 2HSO_3^- \quad (2)$$

accounts for the mass loss of dithionite that cannot be used for iron reduction. Previous studies have shown that this reaction has a half-life of ~27 h (basaltic sediments). The consequence of this reaction is to limit how slowly dithionite can be reacted with (i.e., injected into) sediment in the field. If dithionite is injected too slowly, a significant amount of the mass is lost to disproportionation (Chilakapati et al. 2000). Although iron(III) phases are the most significant phase that reacts with dithionite, other mineral phases present in natural sediments may also be reduced and use some of the dithionite. Previous studies have shown that some Mn reduction occurs as a result of the dithionite treatment of Hanford sediment, although reduced Mn^{II} phases were only 3 to 4% relative to reduced iron phases.

2.2 Sediment Oxidation Mechanisms

The oxidation of the adsorbed and structural Fe(II) in the sediments of the permeable redox barrier occurs naturally by the inflow of dissolved oxygen through the barrier, but can additionally be oxidized by contaminants that may be present such as chromate, TCE, nitrate, uranium, or other electron acceptors. If redox equilibrium completely defined the mechanism (i.e., no effects from activation energies or surface catalysis), and contaminants are present in equal molar concentrations, they would be reduced in the following order:

$$\text{chromate} > \text{dissolved oxygen} > \text{nitrate} > \text{uranium} > \text{pertechnetate} > \text{TCE} \quad (3)$$

In most aquifers, dissolved oxygen in water is the dominant oxidant of reduced iron species, as contaminants are generally present in lower molar concentrations relative to dissolved oxygen (Vermeul et al. 2000). The oxidation of reduced iron in pure mineral phases is described by the following reactions first by dissolved oxygen, then with other contaminants. Fe(II) species that are known to exist in the dithionite-reduced sediments include adsorbed Fe(II) and siderite [$Fe(II)CO_3$]. A single mole of electrons is consumed as a mole of these species are oxidized:

$$Fe^{2+} <==> Fe^{3+} + e^- \quad Eh = -0.771 \text{ v} \tag{4}$$

$$FeCO_3(s) + 3H_2O <==> Fe(OH)_3(s) + 2H^+ \; HCO_3^- + e^- \tag{5}$$

The use of dissolved oxygen as an oxidant is generally divided into two electron sequences, which combined:

$$O_2 + 4H^+ + 4e^- <==> H_2O, \quad Eh = 1.23 \text{ v} \tag{6}$$

show that 4 moles of electrons are needed per mole of O_2 consumed. The rate of this reaction (6) has generally been observed to be first-order at fixed pH, and the rate increases a hundredfold for a unit increase in pH. Experimental evidence during iron oxidation experiments indicates that two differing reduced iron species are present (adsorbed ferrous iron and siderite). Combining the two iron oxidation half reactions with oxygen reduction:

$$4{\equiv}Fe^{2+} + O_2 + 4H^+ <=> 4{\equiv}Fe^{3+} + H_2O \quad Eh = -1.85 \text{ v} \tag{7}$$

$$4{\equiv}FeCO_3(s) + O_2 + 4H^+ <=> 4{\equiv\equiv}Fe^{3+} + 2\,H_2O + 4CO_3^{2-} \tag{8}$$

yields 4 moles of Fe(II) oxidized and 4 moles of electrons transferred per mole of O_2 consumed. At oxygen-saturated conditions (8.4 mg L^{-1} O_2, 1 atm, 25˚C), 1.05 mmol L^{-1} Fe(II) is consumed. Experimental evidence indicates that the oxygenation of Fe(II) in solutions (pH >5) is generally found to be first order with respect to Fe(II) and O_2 concentration and second-order with respect to OH-. The rate of oxidation of aqueous Fe^{2+} by oxygen at pH 8 is a few minutes (Eary and Rai 1988; Buerge and Hug 1997). In contrast, the oxidation rate (as a half-life) observed in natural sediments [surface Fe(II) phases mainly adsorbed Fe(II) and $Fe(II)CO_3$] was found to be 0.3 to 1.1 h.

When contaminants are present at high concentration, their impact on iron oxidation needs to be considered. The reduction of 1 mole of chromate oxidizes 3 moles of Fe(II), or 41 mg L^{-1} chromate is needed to oxidize the equivalent mass of Fe(II) as water saturated with dissolved oxygen [1.05 mmol L^{-1} Fe(II)]. The degradation of TCE to ethylene by reductive elimination consumes 5 moles of electrons, or 26 mg L^{-1} TCE is needed to oxidize the equivalent mass of Fe(II) as water saturated with dissolved oxygen. Nitrate reduction consumes 2 moles of electrons, or 67 mg L^{-1} nitrate has the equivalent oxidation capacity as water saturated with dissolved oxygen. RDX degradation consumes 8 moles of electrons (to the fourth product, minimum observed in this study) or 24 moles of electrons to achieve mineralization. Therefore, RDX is likely a major oxidant limiting the barrier longevity, as 33 mg/L RDX (assuming 8 electrons) or 10 mg/L RDX (assuming 24 electrons) consumes the equivalent electrons as O_2-saturated water.

2.3 RDX Abiotic and Biotic Degradation in Sediments

The most fundamental unanswered question is whether any pH/Eh conditions (such as reducing conditions) in sediments can *abiotically* destroy RDX. Although the degradation pathway for RDX with Fe^0 is largely complete (Singh et al. 1998, 1999), the pathway in reduced natural sediments is unknown. The abiotic pathway may initially be similar to RDX biotic degradation, with reduction of nitro groups (Figure 2.1). RDX abiotic degradation experiments with Fe^0 (Singh et al. 1999) have shown that an Eh of -150 mV is needed to induce redox reactions, but more highly reducing conditions did not increase the rate. The RDX biotic degradation pathway (Figure 2.1) under reducing conditions proceeds by a step-wise reduction of the three nitro-functional groups (i.e., $-NO_2$-> -NO -> -NHOH), where each of these reactions consumes two electrons. Approximately 26 different biotic reaction products have been identified or hypothesized (McCormick et al. 1981; Hawari 2000), although not all reaction intermediates have been identified.

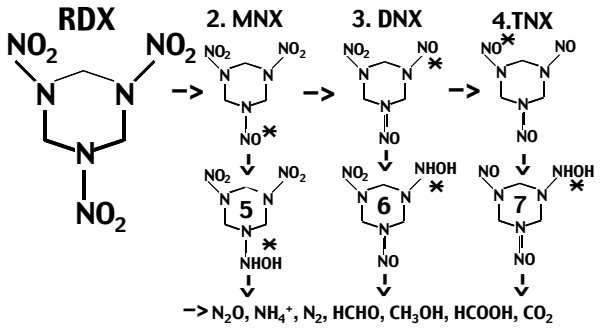

Figure 2.1. RDX Biotic Degradation Path

In this study, the first four compounds were identified by high performance liquid chromatography (HPLC) analysis (RDX, MNX, DNX, TNX, and there were some measurements of a final product, carbon dioxide. Reaction modeling was used to determine reaction rates and influence of sorption. The first four reduction reactions by ferrous iron are:

$$RDX + 2Fe^{2+} <=> MNX + 2Fe^{3+} + 2OH^- \quad (9)$$

$$MNX + 2Fe^{2+} <=> DNX + 2Fe^{3+} + 2OH^- \quad (10)$$

$$DNX + 2Fe^{2+} <=> TNX + 2Fe^{3+} + 2OH^- \quad (11)$$

$$TNX + 2Fe^{2+} <=> un1 + 2Fe^{3+} + 2OH^- \quad (12)$$

where RDX is hexahydro-1,3,5-trinitro-1,3,5 triazine; MNX is hexahydro-1-nitroso--3,5-dinitro-1,3,5triazine; DXN is hexahydro-1,3-dinitroso--5-nitro-1,3,5triazine; TNX is hexahydro-1,3,5-trinitroso-1,3,5triazine; and un1 (unknown 1 by HPLC analysis) may be a noncyclic compound such as #8 on the

degradation path (McCormick et al. 1981; N-hydoxymethylmethylenedinitro-amine). For the purpose of modeling, it is necessary to consider the electron consumption to obtain carbon dioxide, so:

$$un1 + 14Fe^{2+} <=> CH_3NHNHCH_3 + MeOH + HCHO\ 14Fe^{3+} + 14OH^- \quad (13)$$

where $CH_3NHNHCH_3$ (1,2-dimethylhydrazine) is considered the final product. HCHO is then converted into acetic acid (acetogens) then methane and carbon dioxide (by methanogens; Hawari 2000). The total electron consumption to convert 1 mole of RDX into 0.5 moles of carbon dioxide is 24, so corresponding greater molar quantities of adsorbed ferrous iron are needed to degrade RDX.

3.0 Experimental and Modeling Methods

3.1 Batch and Column Experiments

3.1.1 Quantification of RDX and Products

RDX, MNX, DNX, and TNX were measured in aqueous solution by liquid chromatography. In this HPLC method, 50 mL of sample were injected into an aqueous stream of 60% water and 40% methanol at a flow rate of 0.8 mL/min into a C-18 phase bonded silica column (ThermoHypersil 255-901, 250 x 4.6 mm). Detection was by UV absorption at 235 nm with retention times of 6.33 min (TNX), 7.22 min (DNX), 8.53 min (MNX), and 9.86 min (RDX). The relative mass of carbon dioxide by mineralization of RDX was quantified by the use of 14C-labeled RDX provided by Dr. Steve Comfort (University of Nebraska, Lincoln) by liquid scintillation counting. Iron extractions conducted on untreated and dithionite-treated sediments (Heron et al. 1994) in an anaerobic chamber consisted of: a) 1 M $CaCl_2$ (Fe^{II} ion exchangeable), b) 0.5 M HCl, c) NH_2OH, HCl, and d) dithionite-citrate-bicarbonate (DCB). Aqueous Fe^{II} and Fe^{III} from extractions were quantified by ferrozine. The $Fe^{II}CO_3$/FeS was defined by the 0.5 M HCl minus the 1 M $CaCl_2$ extraction. Amorphous and poorly crystalline Fe^{III} oxides were defined by the NH_2OH, HCl extractions, and crystalline Fe^{III} oxides were defined by the DCB minus the NH_2OH, HCl extraction.

3.1.2 RDX Batch and Column Studies

Well-characterized Ft. Lewis (Tacoma, Washington; Szecsody et al. 2000b) and Pantex sediments corrected by site personnel (Zone 7 near Playa 3, core PTX06-1057, unperched aquifer 253- to 258-ft depth) were used to conduct time-course RDX degradation pathway and rate studies in batch systems (Szecsody et al. 2000a). These experiments consist of a series of steps: a) sediment reduction by sodium dithionite for 48-120 h; b) addition of reduced sediment and RDX-laden water to glass, septa-top vials under anaerobic conditions; and c) measurement of RDX and degradation products of the aqueous solution at specified times. Typically, 20 mg/L RDX was used in experiments. Samples were analyzed at times ranging from 30 s to 1,000 h. Radiolabeled (^{14}C RDX) experiments were also conducted by a similar method, but with an additional glass trap hanging in the batch septa-top vials. These traps contained 0.25 mL of 0.6 mol/L KOH. At specified times, the aqueous solution and reduced sediment was acidified (0.5 mL of 1 mol/L HCl) and after 48 h the KOH was extracted from the trap without uncapping the vial (with a needle through the septa) and counted for 14C-labeled carbon dioxide. The purpose of maintaining the vial seal was to keep gas phase reaction products in the system. In some cases, aerobic experiments were then conducted in the same vials, which may have included degradation of gas phase components. This step involved vials that were not acidified, but at specified times, the KOH in the trap was removed (i.e., to measure abiotic anaerobic mineralization), new KOH added, and 4 mL of air injected into the vial. After an additional 200 h, the second KOH trap was removed and 14C carbon dioxide measured to quantify abiotic aerobic degradation. In one-column studies, some effluent vials were used to conduct batch biotic degradation experiments. In this case, fresh sediment was initially present in an aerobic vial that the effluent was injected from the abiotic anaerobic column.

RDX sorption to sediments is relatively minor (K_d values <2 cm^3/g). However, the combination of sorption and degradation may involve some influence of sorption on the RDX degradation rate. RDX sorption experiments were conducted over a concentration range of 0.04 mg/L RDX to 25 mg/L (roughly half the solubility). RDX photodegradation was addressed (fluorescent light only) to ensure that time course experiments were not being influenced. RDX biodegradation in the natural aerobic sediment (nonsterile, sterile) was also tested to account for any natural biodegradation. RDX reactivity with dithionite itself was tested in vials containing water, RDX, and dithionite (no sediment) during these time course experiments.

Small, 1-D column experiments consisted of injecting RDX-laden water into reduced Pantex sediment at a steady flow rate and collecting effluent water for measurement of degradation products. Two column experiments were conducted at a 0.4 and 4.0 h residence time in which RDX and the first three degradation products were measured. The effluent from the column was routed into an automated six-way multiplexing valve, which was connected to five septa-top vials and a waste bottle. The computer-controlled valve alternated between routing effluent to one septa top vial for a specified time (1 to 36 h), then routed effluent to the waste bottle (4 to 72 h). This enabled anaerobic collection of effluent at specified times. The extent of mineralization (carbon dioxide production) was then measured in the same column by injection of 14C-labeled RDX at a residence time of 8.77 h. Effluent was routed to the same six-way multiplexing valve, except septa top vials contained KOH traps, as described above, for 14C carbon dioxide collection.

3.1.3 Sediment Reduction by Dithionite in Batch and Column Systems

Batch vials containing 5 to 20 g of sediment and 50 mL of water were mixed with continuous helium bubbling in an anaerobic chamber for 30 min before dithionite and pH buffer were added. The dithionite solution contained 0.03 to 0.10 mol L^{-1} sodium dithionite ($Na_2S_2O_4$), with 4x the dithionite concentration K_2CO_3, and 0.4x $KHCO_3$. The dithionite concentration was measured by UV absorption at 315 nm, as described below. Sediment reduction studies conducted in 1-D columns consisted of injecting the dithionite solution at a steady rate into a sediment column and measuring the concentration of dithionite over time in the effluent for 48 to 160 h. The flux rate was chosen to achieve specific residence times of the dithionite solution in the column (2 to 4 h) relative to the reduction rate (~5 to 7 h). The dry bulk density and porosity of the column was calculated from the dry and saturated column weight and column volume. The volumetric flow rate was calculated from the effluent volume and elapsed time. The electrical conductivity of the column effluent provided a second (dynamic) measure of the porosity, and was measured using a flow-through electrode and automatic data logging.

The dithionite concentration in the effluent was measured once per hour using an automated fluid system and data logging equipment. These measurements were taken with an HPLC injection valve with 15 to 52 µL loop that isolated a specified volume of the effluent. The contents of the loop were mixed with 5 to 10 mL of oxygen-free water, then injected into a UV-detector and absorbance measured at 315 nm. The sample injection took 2 min to flow the complete sample through the detector, and the absorbance over a 1-min interval was averaged for a single dithionite concentration measurement. A triple-wash between injections prevented sample overlap. These fluid operations were controlled from one computer and the dithionite concentration logged on a second computer. The concentration of the

dithionite influent was measured with the same automated system by manually bypassing the column at approximately 24 h intervals over the multi-day experiments. The fraction of reduced iron was calculated from dithionite breakthrough curves by determining the total mass loss (i.e., dithionite mass injected minus dithionite in the effluent) and the mass of dithionite used for disproportionation. The remaining dithionite mass loss was used for iron reduction. This dithionite breakthrough analysis assumes that dithionite has reached a steady state mass loss due to disproportionation and that all the iron has been reduced. The rate of iron reduction is also calculated from the steady state dithionite concentration during initial breakthrough (i.e., before the iron is all reduced).

3.1.4 Sediment Oxidation in Columns

Sediment oxidation studies were also conducted in 1-D columns to determine the rate at which the dithionite-reduced sediments are oxidized and to measure of the mass of reduced iron (i.e., redox capacity). These experiments consisted of injecting oxygen-saturated (8.4 mg L^{-1}) water at a steady rate (typically 2 pore volumes per hour) into a reduced sediment column and measuring the concentration of dissolved oxygen over time in the effluent for 100 to 800 h. A series of in-line micro-electrodes were used to monitor geochemical changes during oxidation and included dissolved oxygen (2 electrodes), Eh, pH, and electrical conductivity. Electrode measurements were continuously monitored, averaged, and data logged at 2- to 5-min intervals. Two-point calibration was conducted on the in-line oxygen electrodes at 4 to 8 h intervals (oxygen-free and oxygen-saturated solution for oxygen) using an automated fluid system. Electrode data from calibrations were also data logged. The mass of reduced iron that was oxidized was calculated from the mass of oxygen consumed.

3.2 Modeling RDX Abiotic Degradation

Batch experiments provided data showing the decrease of RDX by reduced sediment and the sequential increase/decrease of several degradation products. Although the abiotic pathway can be assumed to be the same as the biotic pathway by a qualitative assessment of the data, modeling was used to quantify rates and possible influence of other reactions. Three different models were written to describe RDX degradation (and sorption) reactions in batch systems. The partial differential equations describing the mass fluxes of these 6 to 10 reactions were numerically solved. The same reactions can easily be placed in a reactive transport code, but that task was beyond the scope of this study.

The first model (model 1) describes only the five sequential abiotic degradation of RDX (i.e., reactions 9 to 13), as shown in detail in Appendix F. All reactions were written as thermodynamic reactions (i.e., reversible). Reaction 9 indicates that RDX degradation is a third-order reaction (first order in RDX concentration, second order in ferrous iron concentration). Because some experimental data indicate that the reaction may not be of this stoichiometry, model 2 was written with variable order (i.e., user specified) stoichiometry for the first four reactions (Appendix F). Finally, experimental data also indicated that while RDX and subsequent degradation product mass disappeared, the appearance of a degradation product lagged relative to the disappearance of RDX. One hypothesis was that sorption may account for mass loss with no degradation, so model 3 was written to incorporate the five RDX degradation reactions (reactions 9 to 13) and sorption of RDX, MNX, DNX, and TNX.

4.0 Results

4.1 Sediment Reduction and Oxidation

Two column experiments were conducted with Pantex sediment to assess the dithionite reduction rate during flow and determine the mass of reduced iron. Applicability of this technology to the Pantex site relies on: a) the ability of dithionite to reduce iron phases in Pantex aquifer sediments, and b) RDX degradation rates in the Pantex sediment under field conditions (packed porous media, temperature). Two sediment reduction experiments (one shown in Figure 4.1a, both in Appendix A) were conducted in which dithionite was continuously injected into a Pantex sediment (from the perched aquifer at 258-ft depth) column. These experiments showed that dithionite was consumed by reduction of iron phases (i.e., the effluent concentration was less than the influent concentration for 100+ hours). The concentration at which the dithionite effluent concentration leveled off initially showed that the iron phase reduction rate was ~7 h. The dithionite influent concentration decreased slowly over days as a result of disproportionation in aqueous solution over this long (170-h) experiment.

One dithionite-reduced column was slowly oxidized by air-saturated water over hundreds of hours (Figure 4.1b) to quantify the redox capacity. In this experiment, two oxygen electrodes were continuously monitoring the oxygen concentration of the effluent and recalibrated automatically every 8 h (calibration data in Appendix A). Results showed that oxygen was completely consumed for the first 250 pore volumes, then slowly increased to near (but not equal to) the injection concentration, indicating a small amount of additional redox capacity. Integration of the area of oxygen consumed showed that 72 μmol Fe^{II}/g of sediment was present (i.e., 0.4% Fe^{II}/g), a considerable amount.

Iron extractions were conducted on Pantex sediment to compare with the redox capacity achieved by oxidation in columns and assess mineralogical changes to the sediment. Untreated Pantex sediment contained 17 μmol/g Fe^{II} carbonate/sulfide, no adsorbed Fe^{II}, 6.3 μmol/g amorphous Fe^{III} oxides, and 29 μmol/g crystalline Fe^{III} oxides (i.e., not equivalent to 72 μmol Fe^{II}/g redox capacity observed). Previous studies showed that ~20% of amorphous and crystalline iron oxides are reduced by dithionite. The dithionite-reduced Pantex sediment showed 28 μmol/g Fe^{II} carbonate/sulfide, 0.13 μmol/g adsorbed Fe^{II}, 4.2 μmol/g amorphous Fe^{III} oxides, and 24 μmol/g crystalline Fe^{III} oxides, so the total redox capacity could not be accounted for in these iron extractions. Further extractions should be conducted to confirm these results. It is also possible that structural iron in smectite clays and/or manganese oxides are responsible for some of the redox capacity observed.

4.2 RDX Abiotic Degradation Pathway and Rate in Batch Systems

Batch studies conducted to determine the RDX reduction pathway by reduced natural sediment demonstrated a similar pathway to biodegradation (McCormick et al. 1981), in which RDX degrades to MNX (hexahydro-1-nitroso--3,5-dinitro-1,3,5triazine), then DNX (hexahydro-1,3-dinitroso--5-nitro-1,3,5triazine), then TNX (hexahydro-1,3,5-trinitroso-1,3,5triazine). Each of these transformations is a

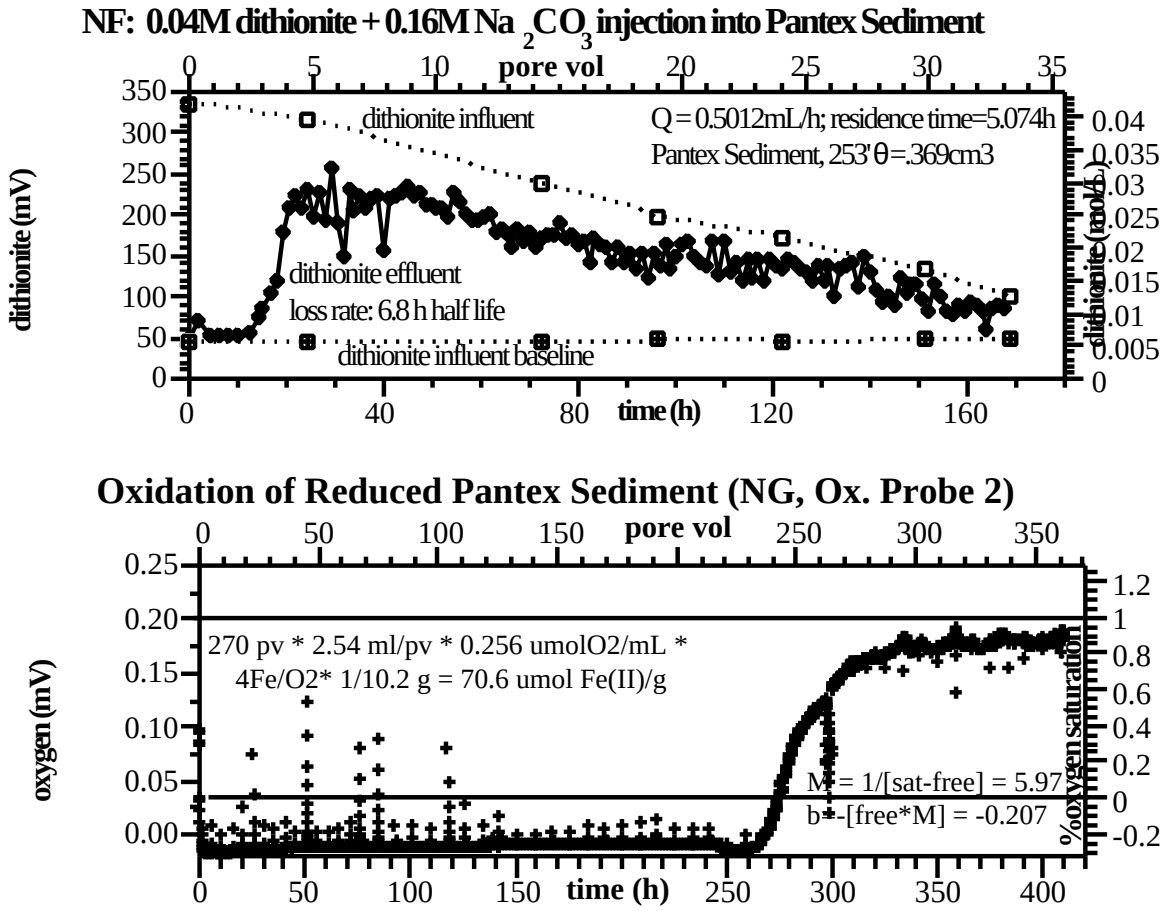

Figure 4.1. (a) Reduction of Pantex Sediment in a Column and (b) Oxidation of Pantex Sediment in a Column

two electron transfer reaction in which a nitro group is transformed into a nitroso group (i.e., -NO_2 to -NO). The pathway is illustrated by batch time-course experiments (Figure 4.2), which shows the evolution of RDX to MNX to DXN to TNX over time.

A total of eight batch time-course experiments were used to quantify the rate of RDX and degradation product transformation in reduced natural sediments. A series of experiments at different sediment/water ratios (two shown in Figure 4.2a and 4.2b) show faster transformation at greater sediment (i.e., Fe(II)) to RDX ratio (i.e., higher soil/water ratio). Data are shown on a log concentration/log time scale to illustrate the species transformations (see Figure 4.2). All experimental data are shown in Appendix B with a linear concentration axis. The observed reaction half-lives in experiments averaged <3 min for RDX to MNX, 0.5 h for MNX to DNX, 10 h for DXN to TNX, and 80 h for TNX to the next product (all at a sediment/water ratio of 1/20). These pseudo-first order rates are not useful for field-scale predictions, as porous media in the Pantex aquifer is at a considerably higher (i.e., 90x) sediment/water ratio. A mathematical model was used to describe the transformation reactions and determine intrinsic rate parameters

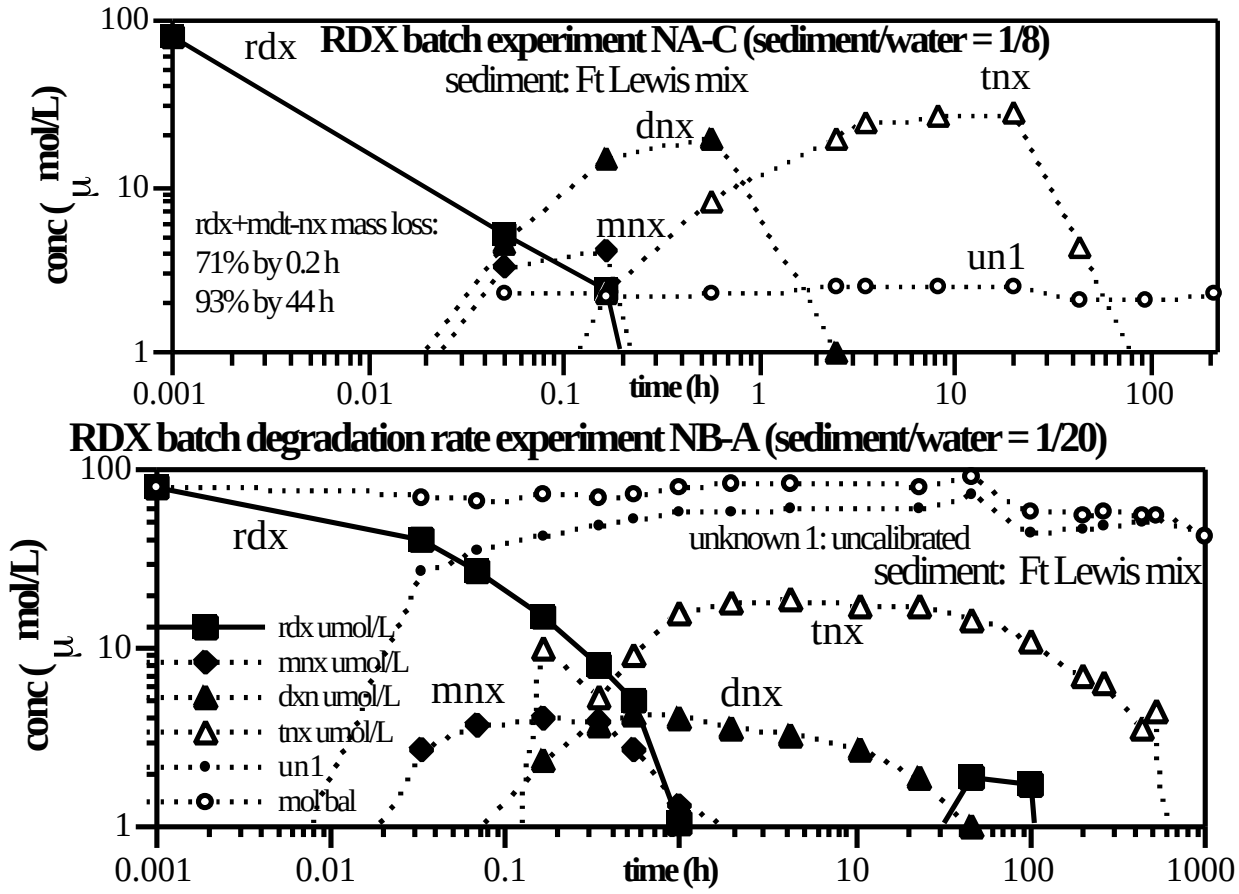

Figure 4.2. RDX Batch Degradation in Dithionite-Reduced Natural Sediments: a) soil/water ratio = 1/8, and b) soil/water ratio = 1/20

that can be used for predictions under differing conditions. Five chemical reactions were used in this model (Table 4.1), which describe five compounds of the ~25 RDX degradation products, using model 1 (RDX sequential degradation, Appendix F) simulations of all batch experiments (Appendix G). One batch RDX degradation experiment was conducted with Pantex sediment (NH, Appendix A), which was not successful. Subsequent column experiments show Pantex sediment does reduce RDX quickly, and reduction experiments show the Pantex sediment is reduced more slowly (Section 4.5). It is likely that sediment in this batch experiment was not fully reduced.

Simulations of the RDX sequential degradation and fit to data (Figure 4.3a to d) demonstrate several key points. First, the mathematical model generally describes behavior (but not completely) where mass balance is fairly good. However, the model generally predicts sooner appearance of a degradation product than is shown by the data. This artifact may be caused by sorption of RDX (and degradation products), which then must undergo desorption before degradation (i.e., resulting in a time lag). That

Table 4.1. Intrinsic Rate Parameters for RDX Degradation from Simulations of Batch Data

Parameter	Value	Half-Life
RDX -> MNX	k_{f1}= 1.3 x 10^5/ (h mol/L), 6 exp.	<3 min
MNX -> DNX	k_{f2}= 1.8 x 10^6/ (h mol/L), 3 exp.	0.5 h
DNX -> TNX	k_{f3}= 3.0 x 10^6/ (h mol/L), 3 exp.	10 h
TNX -> un1	k_{f4}= 4.5 x 10^9/ (h mol/L), 3 exp.	80 h
un1 -> final	k_{f5}= 1.0 x 10^{30}/ (h mol/L), 2 exp.	300 h

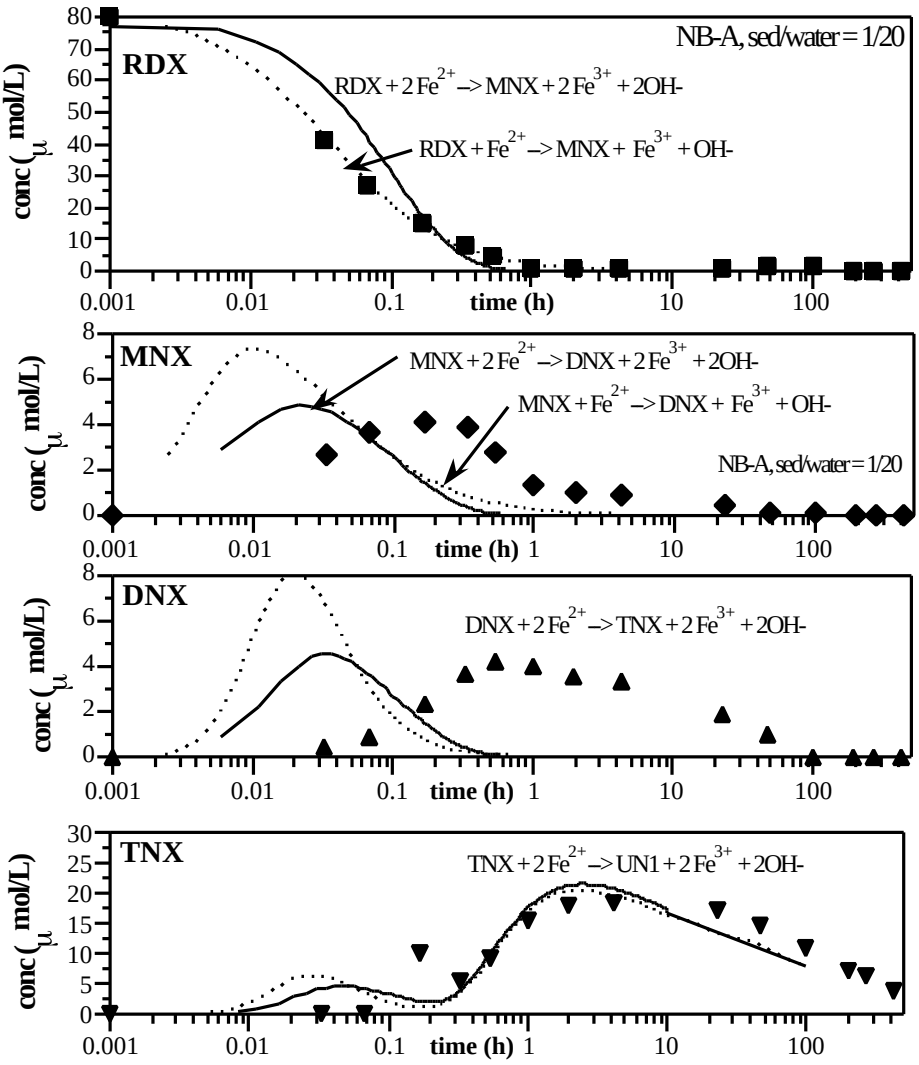

Figure 4.3. RDX Batch Degradation and Model Fit to: a) RDX Data, b) MNX Data, c) DXN Data, and d) TNX Data

concept is further addressed in a later section where sorption is characterized and simulations conducted incorporating sorption. Based on this batch data, the RDX degradation rate at the field-scale soil/water ratio (e.g., and columns) should be <1 sec.

A second concept illustrated by the modeling is the rate dependence on the reaction stoichiometry. As theoretically written, RDX degradation (rxn 9) is a two-electron transfer reaction, with 2 moles of ferrous iron consumed per mole of RDX consumed. That stoichiometry did not fit the rate of RDX consumption (Figure 4.3a, solid line; other simulation fits in Appendix G). Higher order reactions (i.e., this was a second order function of ferrous iron concentration) are generally not found to fit experimental data when surface reactions are involved, so a second model was written (model 2, Appendix F) that incorporates variable order stoichiometry. This allows for the slope of the RDX consumption to be fit (Figure 4.3a) with a first-order stoichiometry (i.e., one mole of RDX and 0.9 mole of ferrous iron). Proof of the actual stoichiometry would require experiments at different reactant concentrations (i.e., rates at differing ferrous iron concentration will show the reaction order). This may be difficult to prove, as it appears that significantly greater ferrous iron concentration on the surface is needed to promote RDX degradation (i.e., there are other catalytic or surface Eh issues other than simple reaction stoichiometry). Furthermore, the variable order model fits to other batch data sets (Appendix G, experiment NAD dashed line; NBB dashed line) were no better than the theoretical stoichiometry (model 1, solid line in all plots). Clearly, in some systems, RDX degradation is slower than predicted as defined only by the simple degradation reaction. This implies additional controls on the RDX reduction rate, such as surface Eh conditions needed to promote the reaction, as found for TCE degradation (Szecsody et al. 2000b) or some other mechanism. In that TCE study, the degradation rate was highly dependent on the fraction of iron that was reduced (i.e., if half of the reducible iron was ferrous iron, the TCE degradation rate decreased an order of magnitude).

The RDX degradation rate was measured as a function of pH, as the rate may increase or decrease depending on the dominant mechanism. The RDX sequential degradation reactions (rxns 9 to 13) should be faster at lower pH. However, the main electron donor (adsorbed Fe^{II}) partitions mainly into aqueous solution at pH <7.5 (i.e., adsorption at higher pH), so a surface-catalyzed reaction should be slower at lower pH. Batch experiments conducted at pH 6 through 10 did not show a trend (Figure 4.4). These experiments were all conducted with a large excess of Fe^{II}/RDX (94:1), which may account for the lack of trend as sufficient adsorbed Fe^{II} may have been available under these conditions over the pH range.

4.3 RDX Abiotic and Biotic Mineralization in Batch Systems

Batch experiments were conducted with Pantex and well-characterized Ft. Lewis sediments to quantify the rate of abiotic and biotic mineralization (carbon dioxide production) under different anaerobic/aerobic conditions. This included: a) abiotic system is always anaerobic; b) abiotic system that is anaerobic for hundreds of hours followed by aerobic conditions; and c) abiotic, anaerobic system for 10 h, followed by biotic, aerobic conditions. The purpose of these differing conditions was to describe RDX mineralization that may occur within a reduced zone in the Pantex perched aquifer, then subsequent abiotic and biotic mineralization that may occur in the aerobic vadose zone below the perched aquifer.

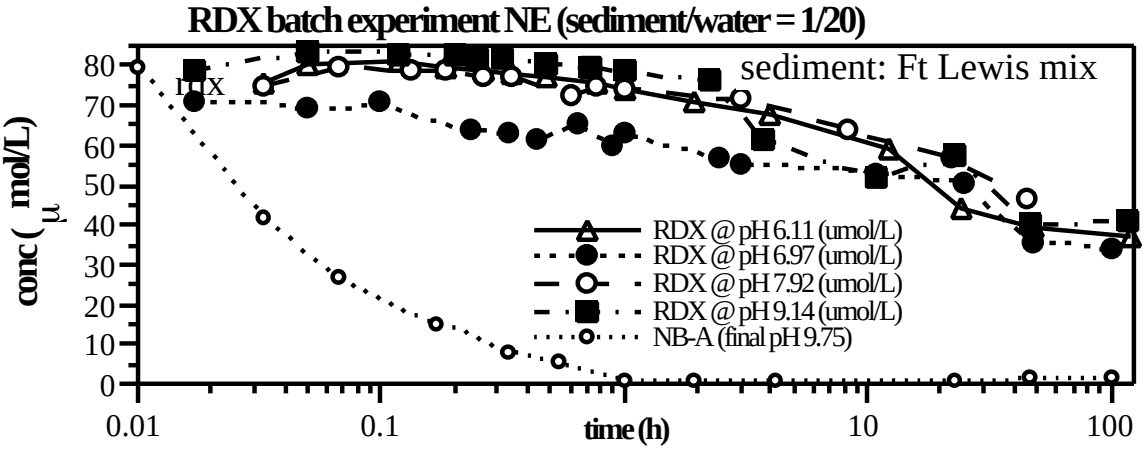

Figure 4.4. RDX Batch Degradation at Different pH

The initial abiotic mineralization studies in anaerobic systems showed very slow carbon dioxide production. After 700 h, three different experiments (Appendix C, experiments NK, NL, NM) showed 2 to 4% mineralization. The Pantex sediment (Figure 4.5a) showed the greatest mineralization. Although a biotic mineralization pathway in totally anaerobic conditions has been observed (Hawari 2000), these are the first data that showed a fully abiotic pathway with some carbon dioxide production in an anaerobic system. Subsequent aerobic mineralization in these abiotic systems (same graphs) indicated some additional mineralization. The Pantex sediment, for example, had an additional 1 to 1.5% mineralization when oxygen was introduced (see Figure 4.5a).

Biotic mineralization following abiotic, anaerobic degradation of RDX was quantified in two separate experiments using effluent from a column experiment described in Section 4.5. In that column experiment, 10 mg/L of RDX was injected into a reduced Pantex sediment column with a flow rate allowing for 8.8 h of reaction time in the column. The RDX was 14-C labeled, and only mineralization was studied in the effluent samples. Effluent was routed into sealed vials containing either only KOH traps (most samples) or fresh Pantex sediment and no additional nutrients (9 samples). In seven samples, both the carbon-14 remaining in aqueous solution and as carbon dioxide were measured. Results of this experiment (Figure 4.4b) show 1 to 1.5% mineralization within the column (i.e., abiotic, anaerobic, 8.8 h), which is considerably faster than observed in the batch experiment. Biotic mineralization under subsequent aerobic conditions (triangles, Figure 4.5b) showed 5% biotic mineralization. The biotic mineralization rate was investigated further in a second batch experiment, which used effluent from this same column (i.e., RDX was degraded to intermediates). This experiment showed biotic mineralization in aerobic systems in the absence of any additional nutrients was still small, but ~10x faster than abiotic mineralization. There was 5% mineralization after 50 h (Figure 4.5c) and up to 20% loss of aqueous carbon-14 (Appendix D, NP plot).

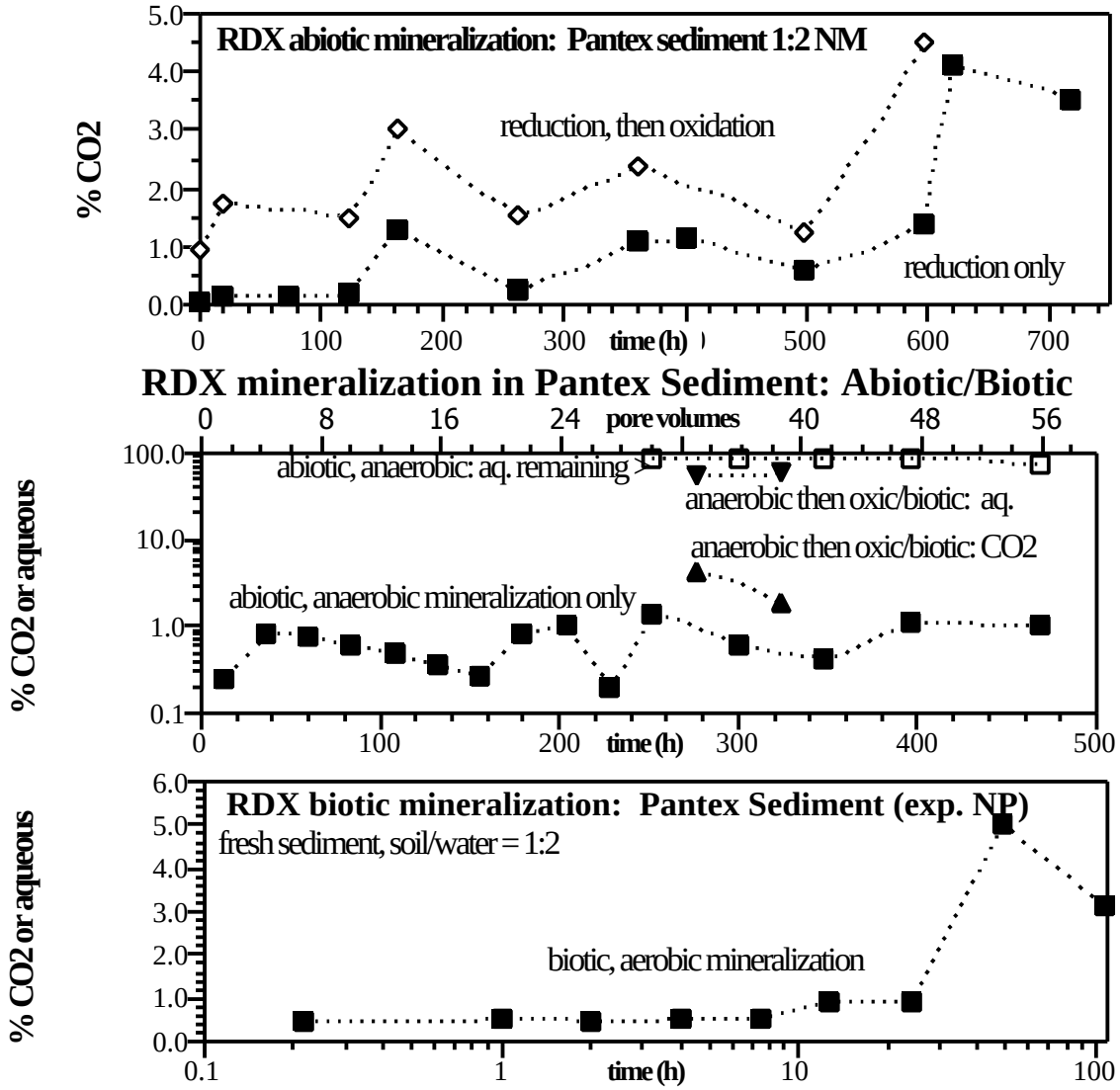

Figure 4.5. RDX Mineralization in a) Batch Abiotic System, Anaerobic and Aerobic, b) Column System, Abiotic Anaerobic and Subsequent Aerobic Biotic, and c) Batch Aerobic System with Fresh Sediment (biotic) and no Additional Nutrients

4.4 RDX Sorption and Other Reactions

Additional batch experiments were conducted to determine the influence of sorption on RDX abiotic degradation. Sorption of RDX to sediment will remove mass, and slow availability for degradation. A sorption isotherm for RDX on Ft. Lewis sediment (Figure 4.6) was fairly linear with no apparent site limitation similar to results of other studies (Ainsworth et al. 1993). Sorption was fairly small, resulting in K_d values ranging from 0.8 cm^3/g at low concentrations (0.05 mg/L RDX) to 0.2 cm^3/g at high

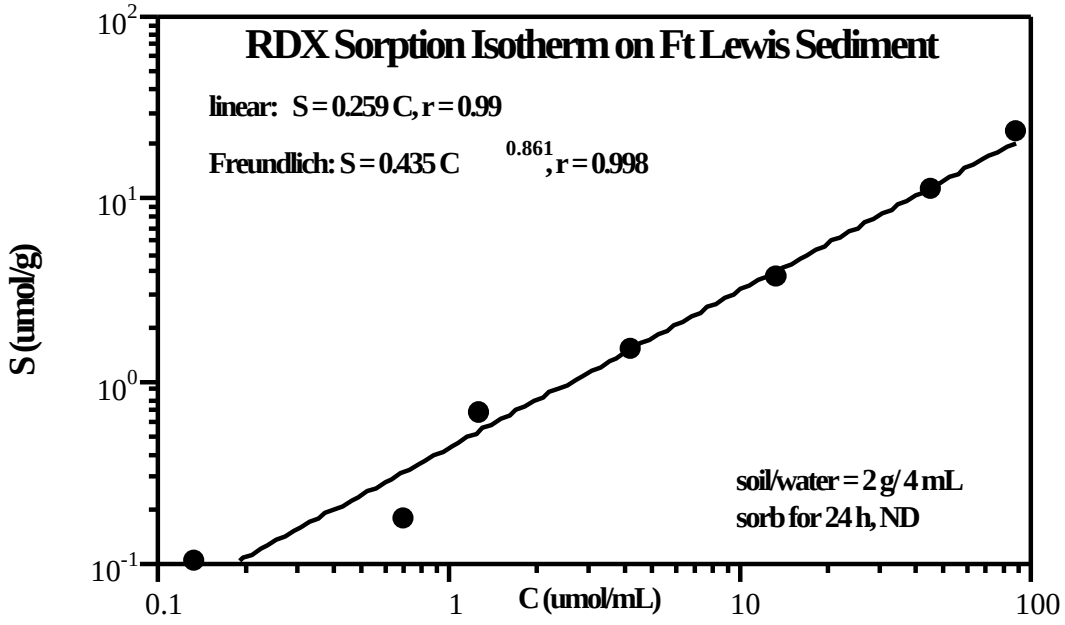

Figure 4.6. RDX Sorption to Oxic Sediment

concentrations (20 mg/L RDX). These values would result in 4% of the RDX mass in batch experiments being sorbed, so could not account for any significant time lag observed in degradation. However, simulation of the influence of sorption (Appendix G, NBA model 1 and NBA model 3) illustrates that there is some time lag (i.e., reaction product appearance lagged 2x in time). Only RDX sorption was measured, but the same 4% sorption was assumed for RDX, MNX, TNX, and MNX.

Sorption in the field, or in packed columns, however, would have ~77% of the RDX mass sorbed, so would result in considerable mass not being available for degradation (i.e., degradation in columns is likely slower than predicted from batch experiments due to sorption). A batch simulation was conducted to illustrate the effect of sorption mass at the column sediment/water ratio (Appendix G, NBA model 3 with column soil/water ratio). The simulation shows rapid disappearance of all species (RDX, MNX, DNX, TNX) due to sorption, and with no adjustment of rates; the RDX disappearance rate would now be dominated by the sorption rate at this high sediment/water ratio.

Additional batch experiments were conducted to ensure that batch RDX degradation results are the result of the reduction by ferrous iron in sediments and not other mechanisms. RDX was reacted with dithionite (experiment NB-CD in Appendix D), which showed that all RDX, MNX, DNX, and TNX is degraded by 1 h. Therefore, RDX degradation does not need to be surface catalyzed, in contrast with TCE degradation. All batch RDX degradation experiments used dithionite-reduced sediment so there may be some (i.e., 3 to 10%) dithionite remaining in the sediment when RDX is introduced; observed rates may by partially a function of the presence of some dithionite. However, dithionite is flushed out of all column experiments, so RDX degradation rates observed in these systems (Section 4.5) are not influenced by dithionite.

Most batch RDX degradation experiments used nonsterile sediment, as previous studies have shown no microbial activity after dithionite treatment (i.e., pH 11 water for 48 to 72 h). The reactivity of RDX in sterile and nonsterile sediment was further tested to look for any reactivity of natural microbes with RDX. This experiment (NC-CD, Appendix D) used 20 mg/L RDX in anaerobic DI water, fresh Ft. Lewis sediment, and 100 mg/L $HgCl_2$ (for sterilization). There was a little microbial activity or abiotic reduction after 200 h with the nonsterile sediment, with up to 3% of the RDX mass as MNX and DNX. In a current study of Tc reduction, natural oxic sediments from the Hanford subsurface had a small amount of available ferrous iron, which reduced pertechnetate. Interestingly, the sterile sediment showed up to 4% of the mass as unidentified RDX degradation products after 300 h. Therefore, RDX biodegradation in nonsterile, dithionite-treated sediment is considered extremely small.

RDX photodegradation in laboratory conditions was tested by a 350-h experiment in which samples exposed to no light (foil wrapped brown vials) and fluorescent light were measured over time (NC-AB in Appendix D). Photodegradation of RDX is an important process in sunlight. There was no degradation measured in either system, indicating clear vials used in all batch experiments were not influenced by photodegradation.

4.5 Transport and Degradation of RDX in Columns

Column experiments were conducted with Pantex sediment to assess RDX degradation under some field-scale conditions. Small 1-D columns represent the soil/water ratio found in the field (i.e., packed porous media), but not natural centimeter or larger scale heterogeneities, as sediment is repacked (although natural mineralogical heterogeneities of iron oxides on grains are present). Three column experiments were conducted at laboratory temperatures (22°C), not field aquifer temperature (15 to 19°C) in the same 15-cm-long column that was reduced by dithionite during flow in experiment NF (Appendix A). RDX was injected at three differing flow rates for a total of 950 h or 257 pore volumes. The Pantex sediment column has 1.6×10^3 times greater ferrous iron than 10 mg/L RDX, so has a theoretical capacity to degrade 660 pore volumes of 10 mg/L RDX to mineralization (i.e., 24 electrons) or 2,000 pore volumes to degrade 10 mg/L RDX to the fourth product (i.e., 8 electrons).

In two column experiments, RDX was injected into the dithionite-reduced sediment column at a flow rate to achieve a residence time of 4.4 and 0.44 h in the column (i.e., reaction time), which is likely 1 to 2 orders of magnitude faster than would be found naturally in the Pantex aquifer. These high flow rates were necessary to collect degradation rate data. In the first experiment (residence time 4.4 h, Figure 4.7a), the 10 mg/L RDX-injected and the first three degradation products were completely degraded within the 4.4 h (i.e., effluent concentrations of these four compounds were below detection limits). This experiment was run for 90 pore volumes (440 h), so there was no influence of dithionite remaining in the column initially. The first sample at 0.91 pore volumes (11 h) contained trace concentration of MNX, but all measurable compounds were removed within the 4.4 h for the next 90 pore volumes.

The second column was conducted with a tenfold faster flow rate (0.44 h residence time) relative to the first column test. This column was run for an additional 110 pore volumes (50 h), and the effluent concentrations quickly leveled off with measurable concentrations of RDX (30% of influent) and TNX (10% of RDX influent mass). This enabled calculation of a RDX removal rate (0.3 h), which is

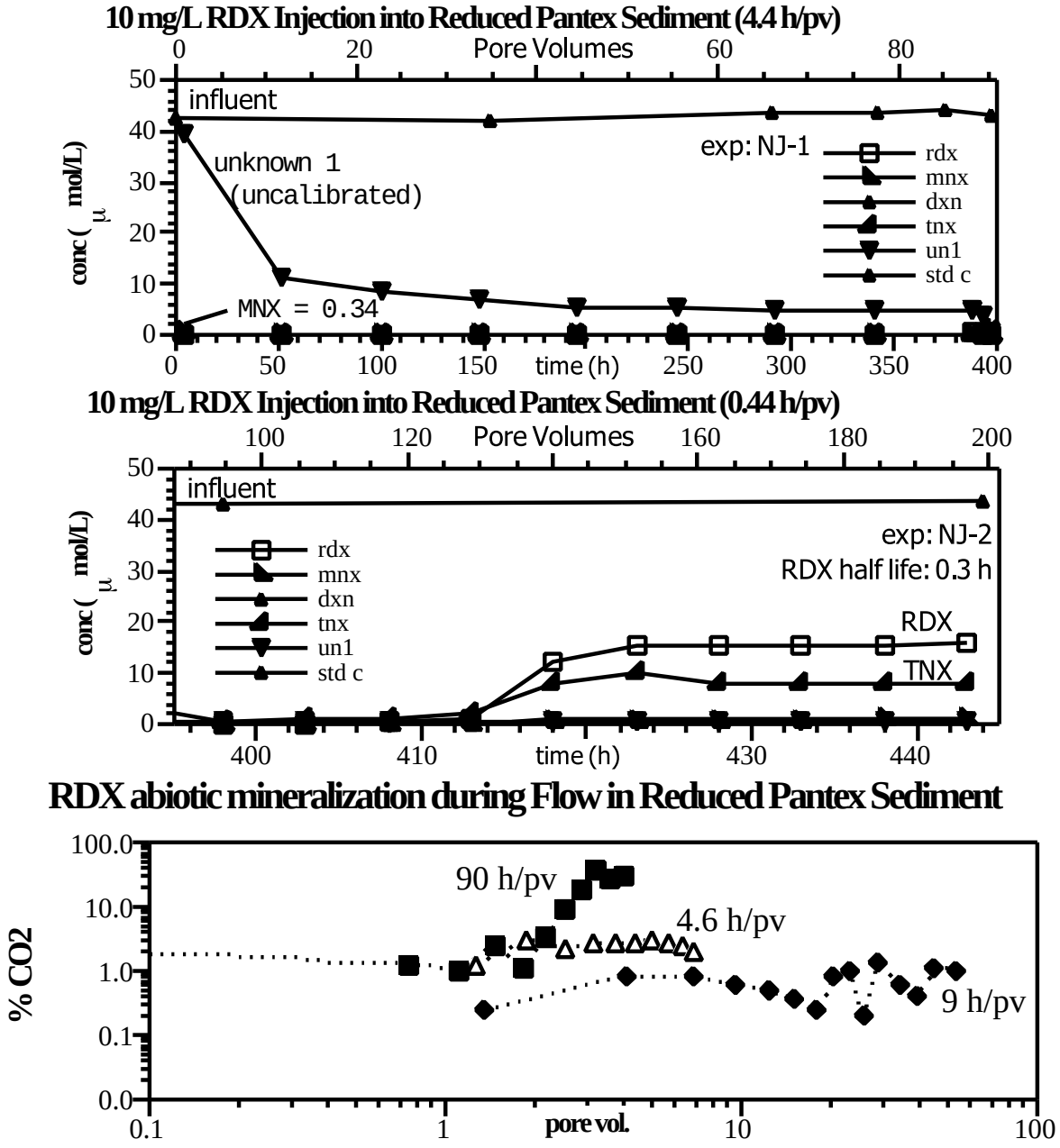

Figure 4.7. RDX Degradation in Pantex Sediment During Flow. The first 90 pore volumes had a residence time of 4.4 h (a), the second 110 pore volumes had a residence time of 0.44 h (b). Mineralization was assessed at three flow rates (c).

considerably slower than predicted from batch data (<1 sec), although the next two products were below detection limits. The third degradation product (TNX) was being quickly degraded (0.17 h half-life, or faster than predicted from batch data). Sorption in columns, removing 77% of the aqueous mass, would have some influence on slowing the RDX degradation rate initially (until sorption equilibrium was

reached), so may account for some of the observed effect. In addition, all aqueous/surface reaction rates are limited by the diffusion rate in aqueous solution. These fairly fast rates show that RDX degradation by dithionite-reduced sediment is a viable technology at the Pantex site. A reduced sediment wall needs to be constructed to achieve a residence time of only a few hours to degrade RDX.

The final RDX column experiments with Pantex were to test the extent of mineralization. In the first of these experiments, ^{14}C labeled RDX is injected into the same Pantex column at a residence time of 8.8 h for 500 h (57 pore volumes). Two additional experiments were conducted on a separate column with residence times of 4.6 h and 89 h. Initial (RDX, MNX, DNX, and TNX) degradation products were not measured on the effluent samples, but aqueous carbon 14 and carbon dioxide concentrations (KOH trap) were measured. The amount of abiotic mineralization was greater with more reaction time: 36% for an 89 h residence time, 1.5% for a 9 h residence time, and 3% for a 4.6 h residence time. This corresponded to a relatively constant abiotic mineralization rate, with a 138 h half-life for the 89 h residence time, and a 101 h half-life for the 4.6 h residence time (Figure 4.7c). The 9 h residence time experiment was considerably slower (640 h residence time), but this column had already been subjected to 240 h of oxidation. Aqueous measurements of the effluent showed 8% and 30% mass loss of aqueous species (Appendix E, experiments NN, NR, and NS). Further mineralization (biotic in aerobic systems, abiotic in aerobic systems) on effluent samples from this third column experiment (2 to 5%) is discussed in Section 4.3.

Results of these three column tests show promising results, illustrating that a reduced Pantex sediment barrier (15 cm long in this case) with even a small reaction time (9 h) can result in the complete and rapid loss of the initial four species (RDX, MNX, DNX, TNX) and additional time (90 h) is needed for significant mineralization (up to 36% observed).

5.0 Conclusions

This laboratory study was conducted to assess RDX (hexahydro-1,3,5-trinitro-1,3,5 triazine) abiotic degradation by chemically reduced sediments and other geochemical aspects of the application of this technology to remediation of RDX contamination in groundwater at the U.S. Department of Energy Pantex facility. Laboratory experiments showed that chemical reduction yielded a fairly high redox capacity (0.4% Fe^{II}/g), which is higher or equal to that achieved at other sites in which field-scale remediation is in progress or being considered (0.1% Hanford 100-D Area, 0.24% Ft. Lewis aquifer, 0.4% Moffett Federal Airfield aquifer, 0.3% Frontier Hard Chrome sediments). This mass of reducible iron represents sufficient quantity to remain anoxic for hundreds of pore volumes in the field, so would last dozens of years, depending on aquifer flow rates and oxygen diffusion.

RDX was quickly degraded (i.e., minutes) in batch studies using abiotic, reduced sediments (iron-reducing conditions) to at least the fourth degradation product. The initial reduction pathway was the same as the biotic pathway (RDX to MNX to DXN to TNX). Simulation of the sequential RDX degradation pathway generally tracked mass fluxes, but indicated that other processes (e.g., sorption) also influenced rates. The rate and extent of *anaerobic* mineralization in these abiotic systems was slow (2% to 4% in 500 h). There was additional *aerobic* abiotic and biotic mineralization (1 and 5%). The importance of the anaerobic/aerobic mineralization is applicable to the Pantex perched aquifer. If RDX can be degraded to some reactions intermediates (as demonstrated), these products will be transported through the vadose zone below the perched aquifer and may be biotically degraded. RDX sorption is small, but may play a role in limiting the fast RDX degradation rate in packed porous media systems. RDX is also quickly degraded by dithionite, illustrating the reduction reaction need not be surface catalyzed. This result is in contrast to TCE degradation, which is not degraded by aqueous ferrous iron, but is degraded by ferrous iron adsorbed to iron oxides, 2:1 smectite clays, and Fe^0.

Pantex sediments degraded RDX quickly in packed columns, which represents idealized flow conditions in the perched aquifer. Degradation rates (half-life) were 18 min for RDX, <1 min for MNX and DXN, and 10 min for TXN. Slow abiotic mineralization was also observed (half-life 100 h). These degradation rates were maintained for 260 pore volumes, further illustrating that a thin reduced sediment barrier with only a few hours of reaction time is needed to achieve the degradation observed. Because anaerobic, abiotic mineralization rates are so slow, the most viable field-scale solution may be initial anaerobic, abiotic degradation of RDX followed by aerobic biotic mineralization, which was observed to be tenfold faster.

In summary, the use of a chemical reductant to reduce iron oxide phases in sediments shows great promise to application to the Pantex perched aquifer. The sediment can be reduced to achieve considerable redox capacity, and RDX is quickly degraded in these reduced sediments. Final applicability depends not only on these geochemical considerations, but additionally on hydrogeologic and injection design considerations to achieve a viable and economic remediation in the deep (260-ft) aquifer.

6.0 References

Ainsworth, C., S. Harvey, J. Szecsody, M. Simmons, V. Cullinan, C. Resch, and G. Mong. 1993. *Relationship between the Leachability Characteristics of Unique Energetic Compounds and Soil Properties*. Final report 91PP1800, U.S. Army Medical Research and Development Command, Ft. Detrick, Frederick, Maryland.

Balko, B., and P. Tratnyek. 1998. "Photo Effects on the Reduction of Carbon Tetrachloride by Zero-Valent Iron." *J. Phys. Chem.* 102(8):1459-1465.

Buerge, I. J., and S. J. Hug. 1997. "Kinetics and pH Dependence of Chromium (VI) Reduction by Iron(III)." *Environ. Sci. Technol.* 31:1426-1432.

Chilakapati, A., M. Williams, S. Yabusaki, C. Cole, and J. Szecsody. 2000. "Optimal Design of an In Situ Fe(II) Barrier: Transport limited reoxidation." *Environ. Sci. Technol.* 34:5215-5221.

Eary, L., and D. Rai. 1988. "Chromate Removal from Aqueous Wastes by Reduction with Ferrous Ion." *Environ. Sci. Technol.* 22:972-977.

Fruchter, J., C. Cole, M. Williams, V. Vermeul, J. Amonette, J. Szecsody, J. Istok and M. Humphrey. 2000. "Creation of a Subsurface Permeable Treatment Barrier Using In Situ Redox Manipulation." *Ground Water Monitor. Rev*. 66-77.

Hawari, J. 2000. "Biodegradation of RDX and HMX: From Basic Research to Field Application." In *Biodegradation of Nitroaromatic Compounds and Explosives*, J. Spain, J. Hughes, and V. Knackmuss (eds.), Lewis Publishers, Boca Raton, pp. 277-310.

Heron, G., C. Crouzet, A. C. Bourg, and T. H. Christensen. 1994. "Speciation of Fe(II) and Fe(III) in contaminated aquifer sediments using chemical extraction techniques." *Environ Sci. Technol.* 28:1698-1705.

Mayer, K., D. Blowes, and E. Frind. 2000. "Reactive Transport Modeling of an In-Situ Reactive Barrier for the Treatment of Hexavalent Chromium and TCE in Groundwater." *Water Res. Res.*, in press.

McCormick, N.G., J. H. Cornell, and A. M. Kaplan. 1981. "Biodegradation of hexahydro-1,3,5-trinitro-1,3,5-triazine." *Applied and Environ. Microbiol.* 42(5):817-823.

Singh, J., S. D. Comfort, and P. J. Shea. 1999. "Iron-Mediated Remediation of RDX-Contaminated Water and Soil Under Controlled Eh/pH." *Environ. Sci. Technol.* 33:1488-1494.

Singh, J., S. D. Comfort, and P. J. Shea. 1998. "Remediating RDX-Contaminated Water and Soil Using Zero-Valent Iron." *J. Environ. Qual.* 27:1240-1245.

Szecsody, J., A. Chilikapati, J. Zachara, P. Jardine, and A. Ferrency. 1998. "Importance of Flow and Particle-Scale Heterogeneity on CoII/IIIEDTA Reactive Transport." *J. Hydrol.* 209(1-4):112-136.

Szecsody, J. E., J. S. Fruchter, D. S. Sklarew, and J. C. Evans. 2000a. *In Situ Redox Manipulation of Subsurface Sediments from Fort Lewis, Washington: Iron Reduction and TCE Dechlorination Mechanisms*. PNNL-13178, Pacific Northwest National Laboratory, Richland, Washington.

Szecsody, J., M. Williams, J. Fruchter, V. Vermeul, and J. Evans. 2000b. "Influence of Sediment Reduction on TCE Degradation, Remediation of Chlorinated and Recalcitrant Compounds." Chapter C2-6 in *Chemical Oxidation and Reactive Barriers*, ed. G. Wickramanayake, p. 369-376, Battelle Press, Columbus, Ohio.

Vermeul, V., M. Williams, J. Evans, J. Szecsody, B. Bjornstad, and T. Liikala. 2000. *In Situ Redox Manipulation Proof-of-Principle Test at the Fort Lewis Logistics Center: Final Report*. PNNL-13357, Pacific Northwest National Laboratory, Richland, Washington.

Appendix A

Pantex Sediment Reduction and Oxidation Column Experiments

NF: 0.04M dithionite + 0.16M Na_2CO_3 injection into Pantex Sediment

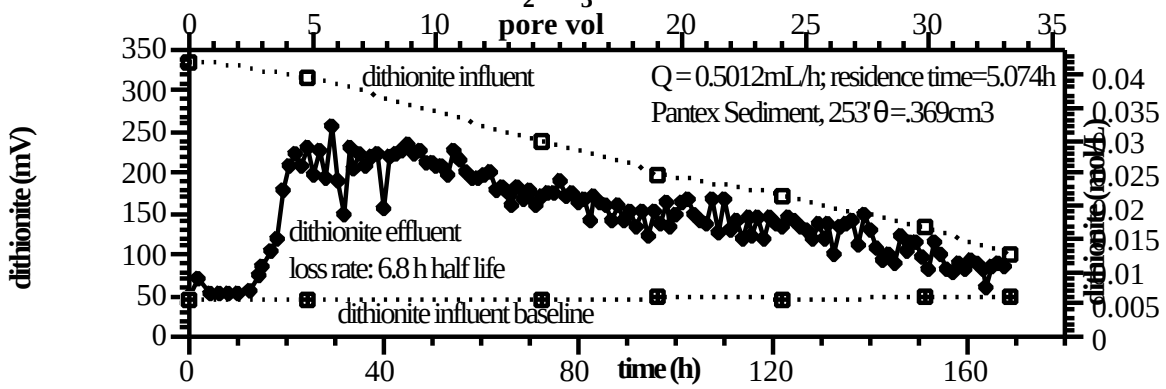

NI: 0.06M dithionite + 0.24M Na_2CO_3 injection into Pantex Sediment

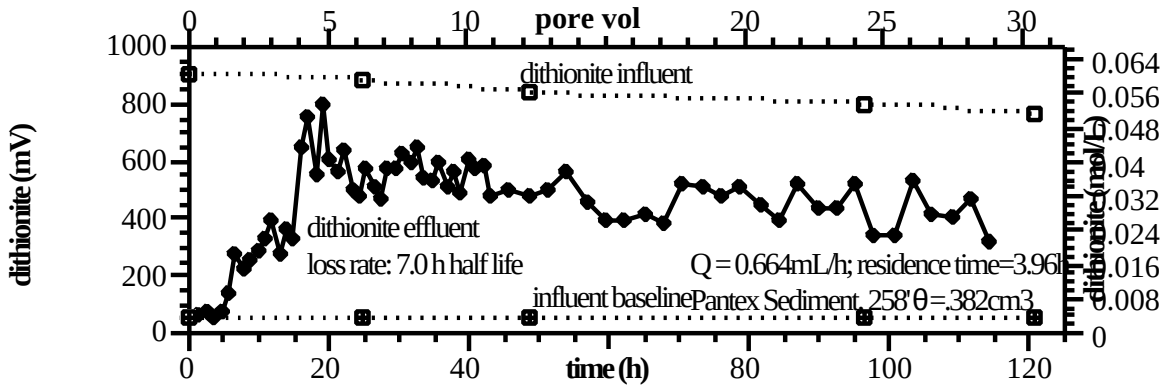

Oxidation of Reduced Pantex Sediment (NG, Ox. Probe 1)

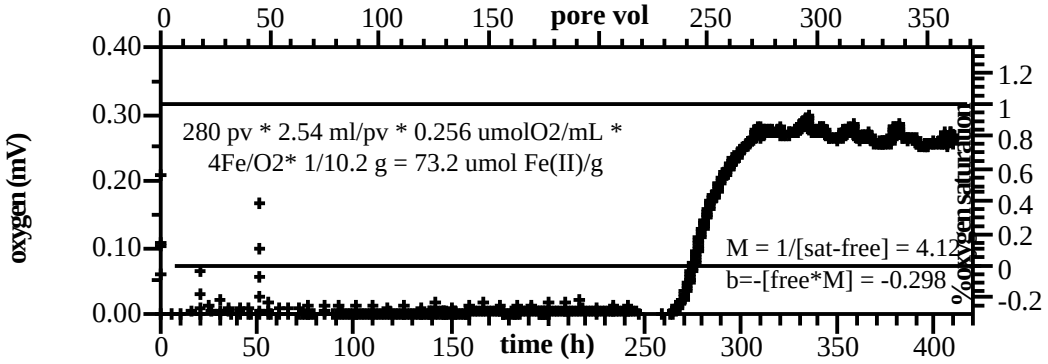

Oxidation of Reduced Pantex Sediment (NG, Ox. Probe 2)

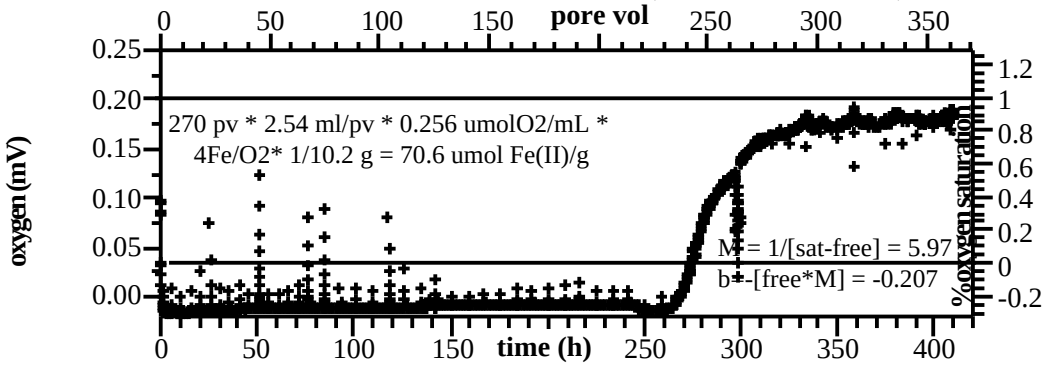

NG: Dissolved Oxygen Stds, Probe 1

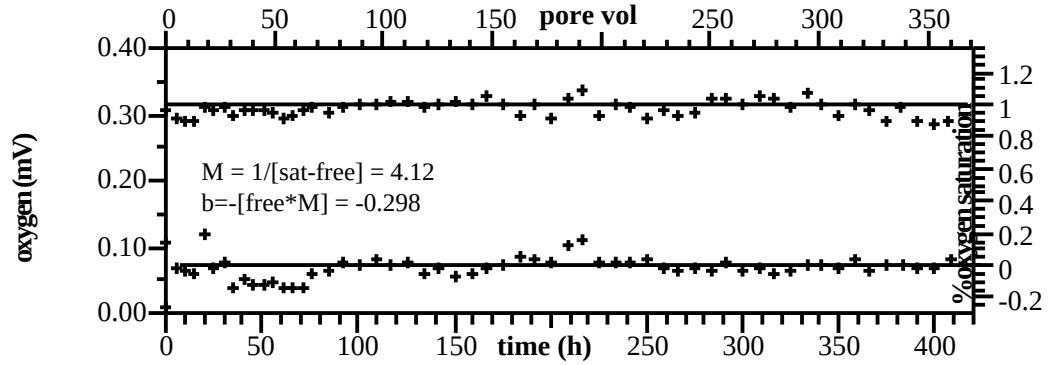

NG: Dissolved Oxygen Stds, Probe 2

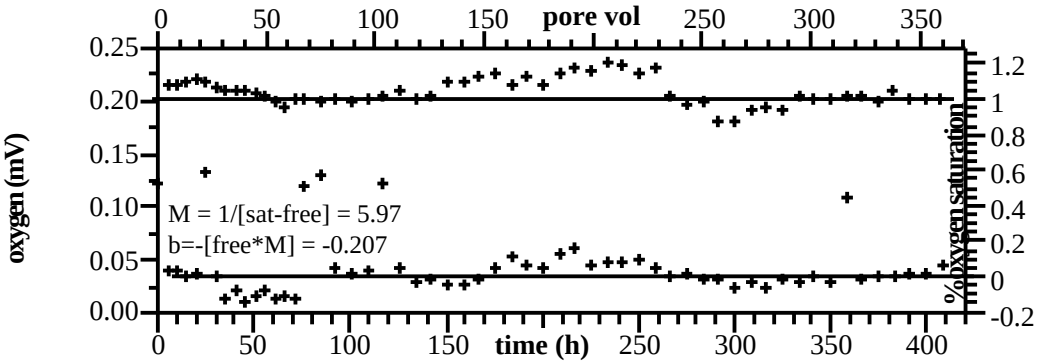

Appendix B

Batch RDX Degradation Rate Experiments

RDX batch degradation rate experiment NA-A (sediment/water = 1/2)

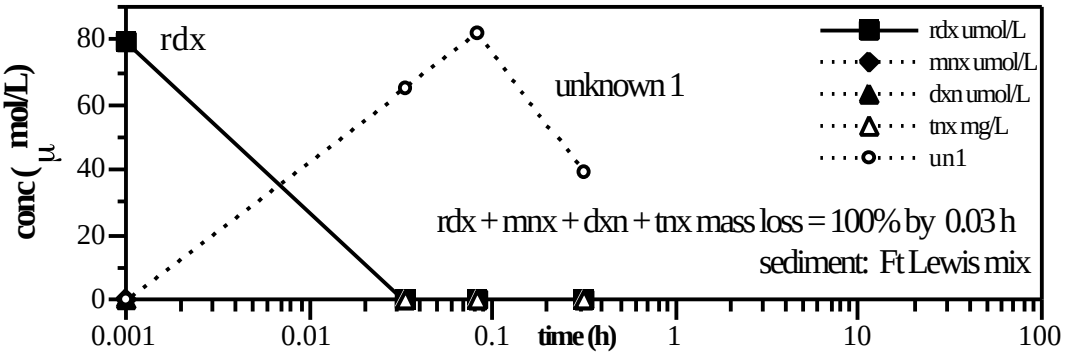

RDX batch degradation rate experiment NA-B (sediment/water = 1/4)

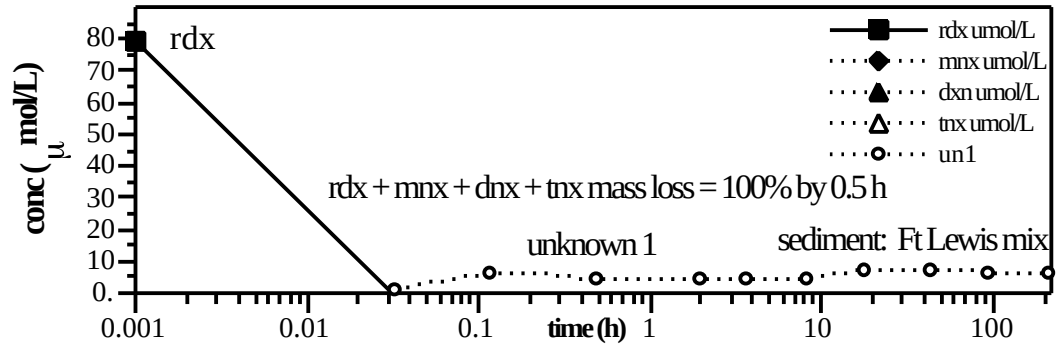

RDX batch degradation rate experiment NA-C (sediment/water = 1/8)

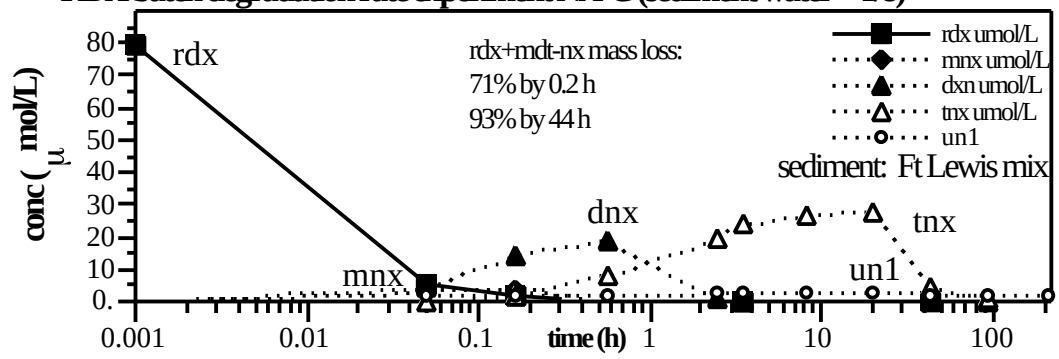

RDX batch degradation rate experiment NA-D (sediment/water = 1/20)

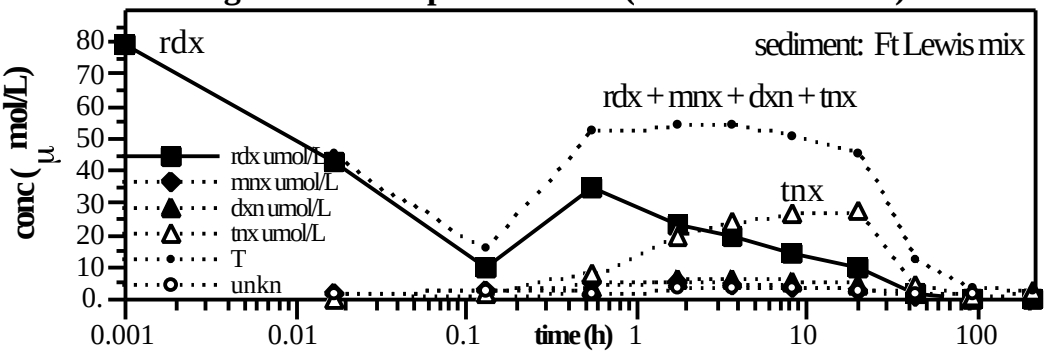

RDX batch degradation rate experiment NB-A (sediment/water = 1/20)

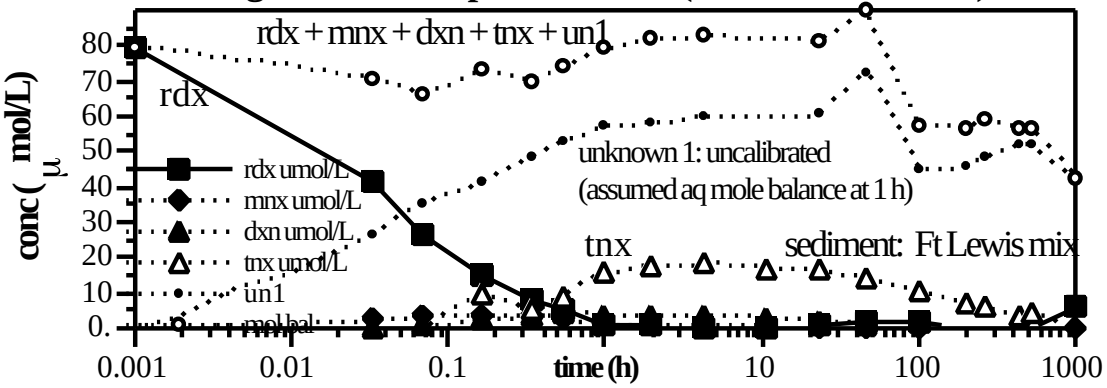

RDX batch degradation rate experiment NB-B (sediment/water = 1/40)

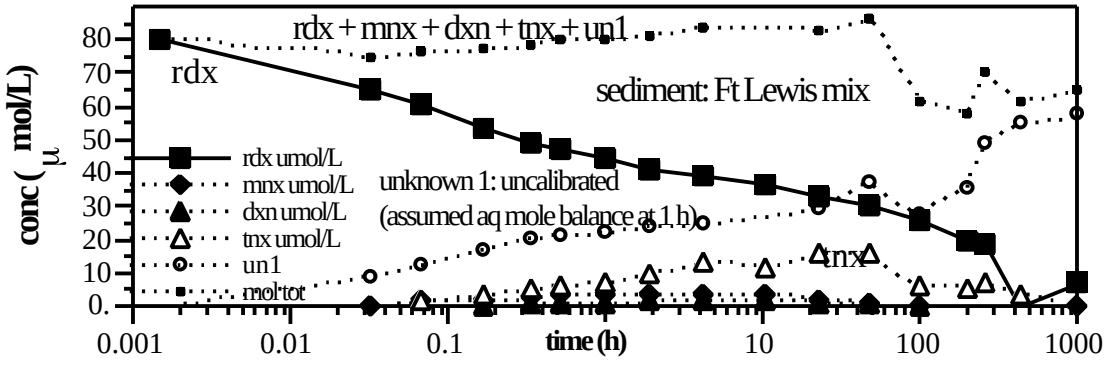

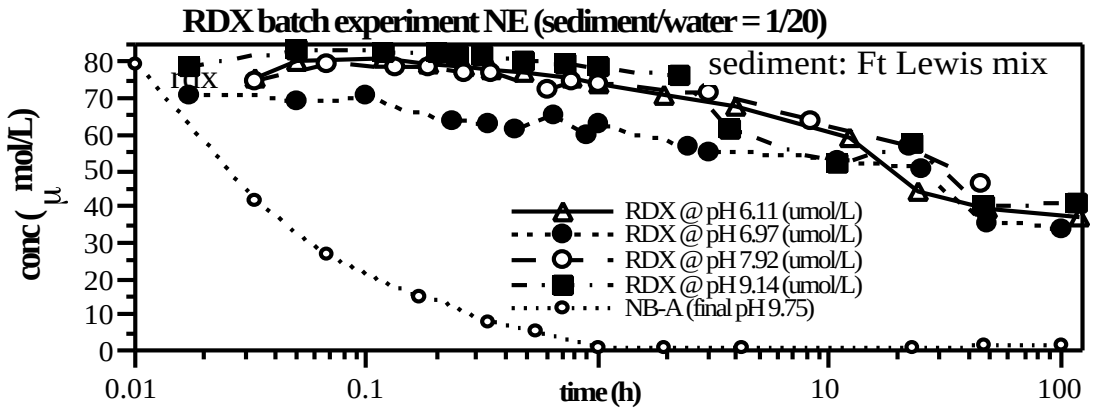
RDX batch experiment NE (sediment/water = 1/20)
sediment: Ft Lewis mix
RDX
RDX @ pH 6.11 (umol/L)
RDX @ pH 6.97 (umol/L)
RDX @ pH 7.92 (umol/L)
RDX @ pH 9.14 (umol/L)
NB-A (final pH 9.75)
conc (μmol/L)
time (h)
0
10
20
30
40
50
60
70
80
0.01
0.1
10
100

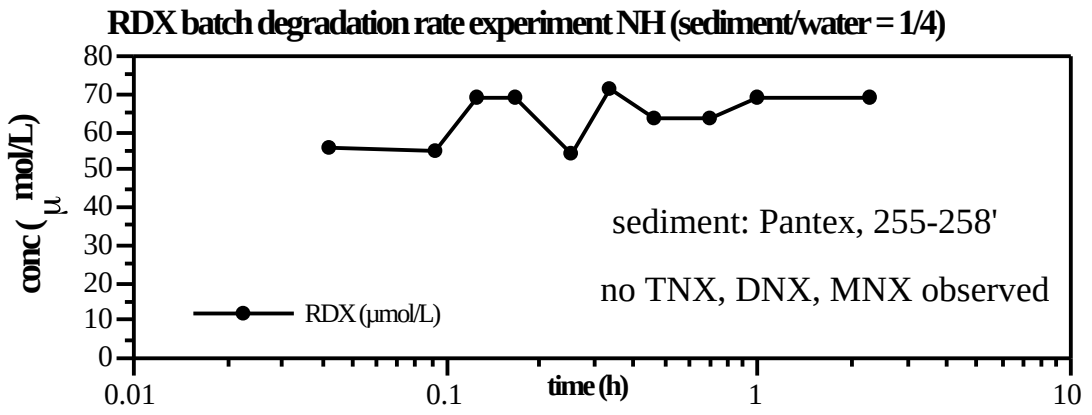
RDX batch degradation rate experiment NH (sediment/water = 1/4)
sediment: Pantex, 255-258'
no TNX, DNX, MNX observed
RDX (μmol/L)
conc (μmol/L)
time (h)
0
10
20
30
40
50
60
70
80
0.01
0.1
1
10

Appendix C

Batch RDX Mineralization Rate Experiments

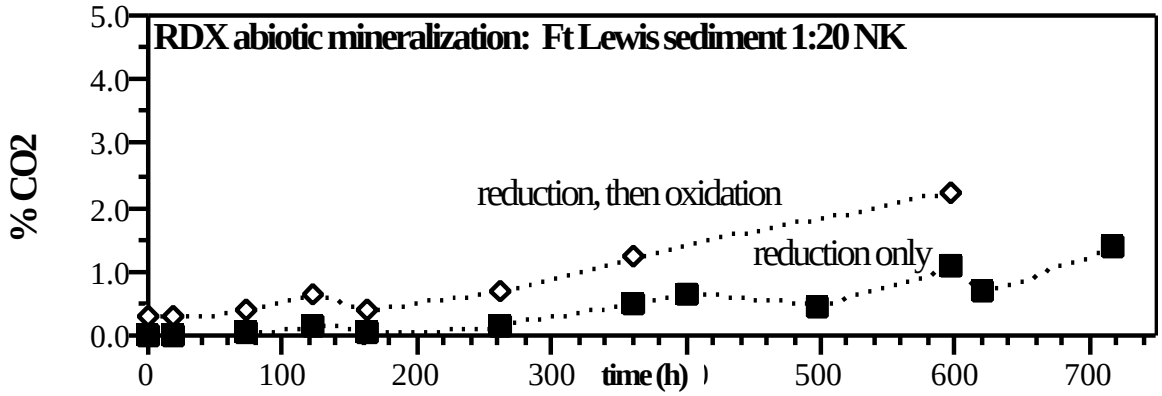
RDX abiotic mineralization: Ft Lewis sediment 1:20 NK
% CO2
5.0
4.0
3.0
2.0
1.0
0.0
reduction, then oxidation
reduction only
0
100
200
300
time (h)
500
600
700

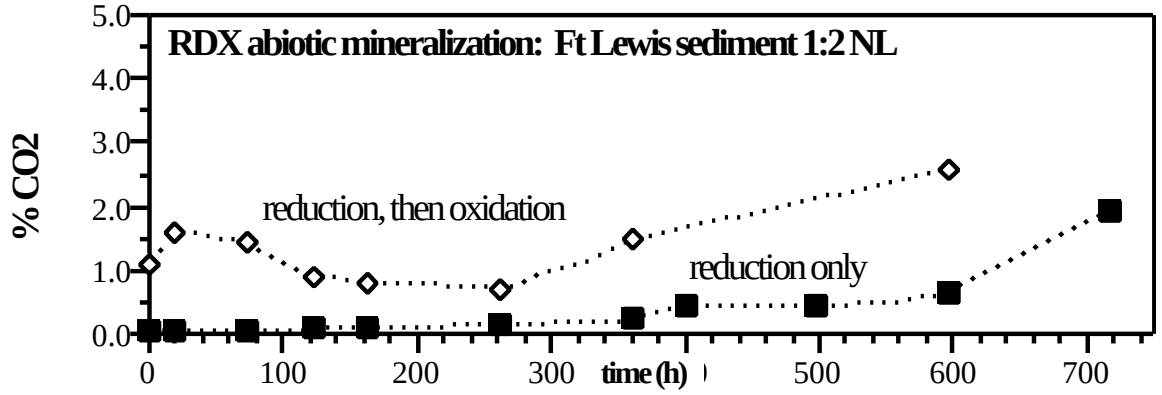
RDX abiotic mineralization: Ft Lewis sediment 1:2 NL
% CO2
5.0
4.0
3.0
2.0
1.0
0.0
reduction, then oxidation
reduction only
0
100
200
300
time (h)
500
600
700

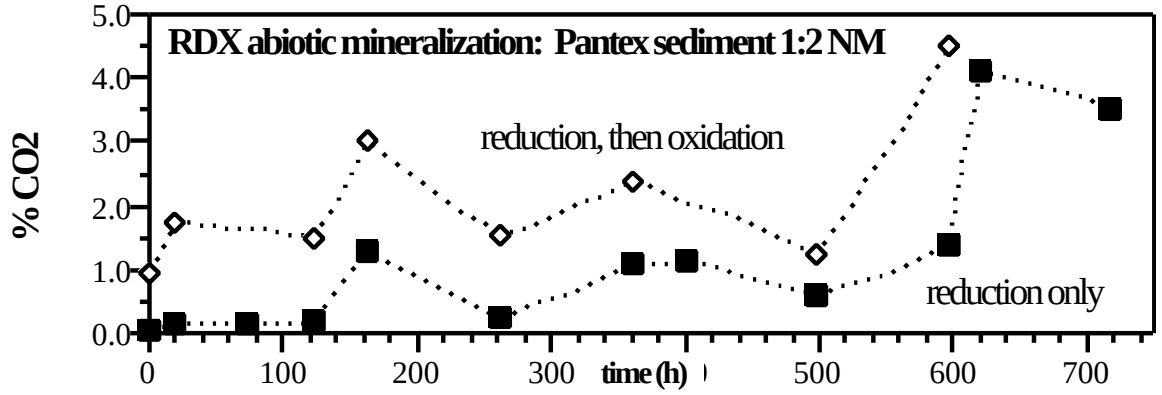
RDX abiotic mineralization: Pantex sediment 1:2 NM
% CO2
5.0
4.0
3.0
2.0
1.0
0.0
reduction, then oxidation
reduction only
0
100
200
300
time (h)
500
600
700

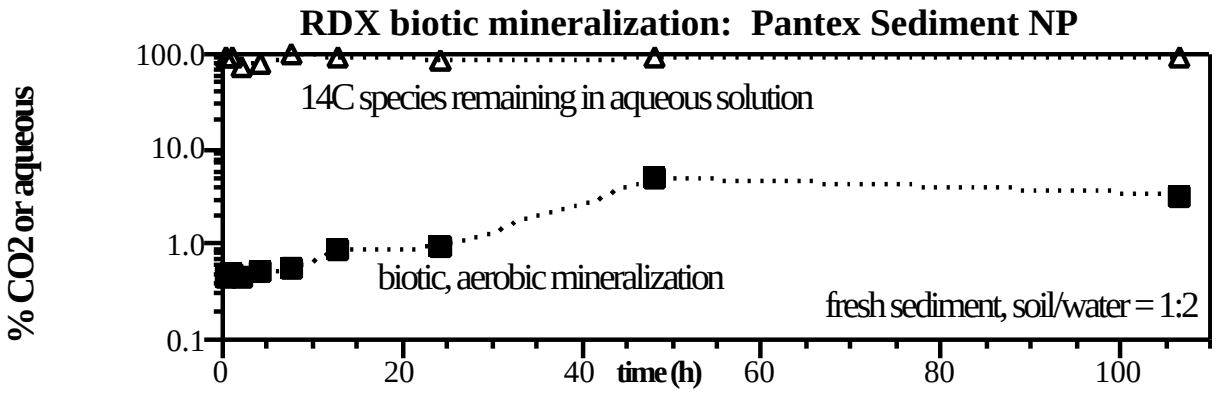
RDX biotic mineralization: Pantex Sediment NP
% CO2 or aqueous
100.0
10.0
1.0
0.1
14C species remaining in aqueous solution
biotic, aerobic mineralization
fresh sediment, soil/water = 1:2
0
20
40
time (h)
60
80
100

Appendix D

Other RDX Batch Experiments

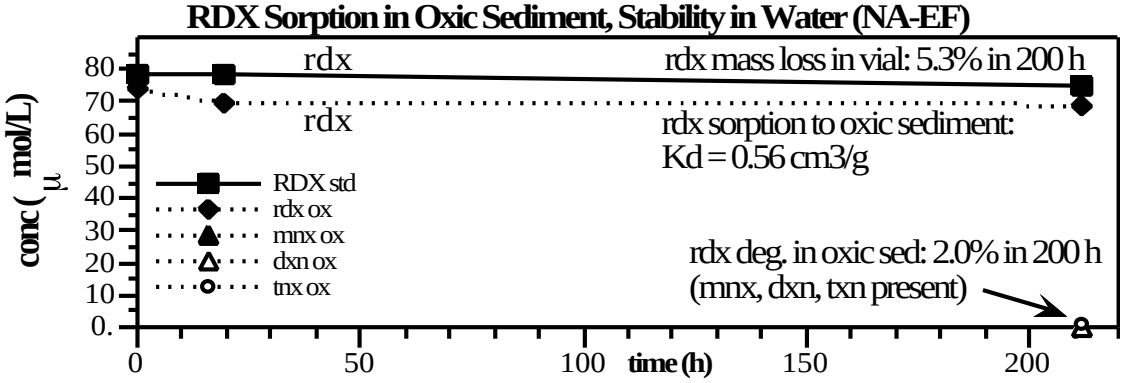
RDX Sorption in Oxic Sediment, Stability in Water (NA-EF)
rdx
rdx mass loss in vial: 5.3% in 200 h
rdx
rdx sorption to oxic sediment:
Kd = 0.56 cm3/g
RDX std
rdx ox
mnx ox
dxn ox
tnx ox
rdx deg. in oxic sed: 2.0% in 200 h
(mnx, dxn, txn present)
conc (µ mol/L)
time (h)

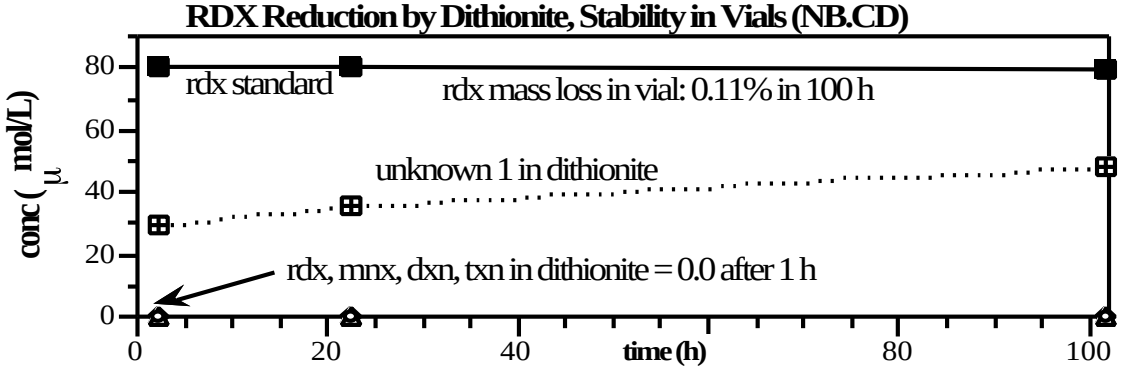
RDX Reduction by Dithionite, Stability in Vials (NB.CD)
rdx standard
rdx mass loss in vial: 0.11% in 100 h
unknown 1 in dithionite
rdx, mnx, dxn, txn in dithionite = 0.0 after 1 h
conc (µ mol/L)
time (h)

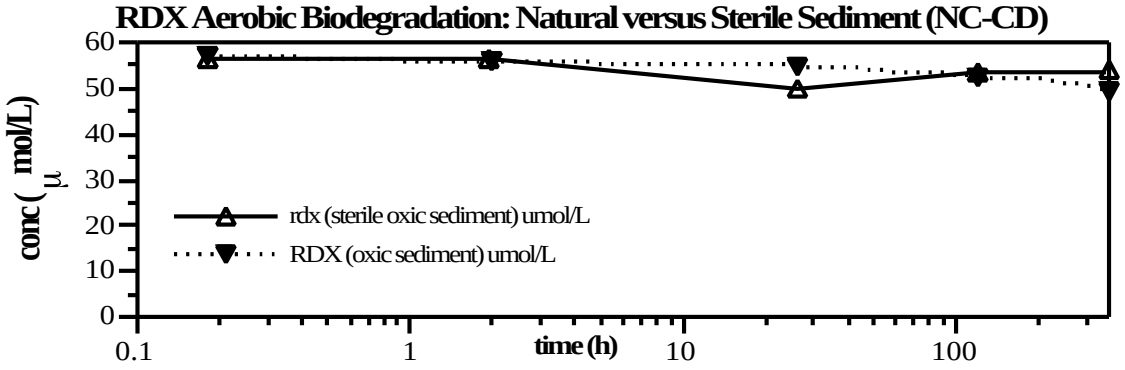
RDX Aerobic Biodegradation: Natural versus Sterile Sediment (NC-CD)
rdx (sterile oxic sediment) umol/L
RDX (oxic sediment) umol/L
conc (µ mol/L)
time (h)

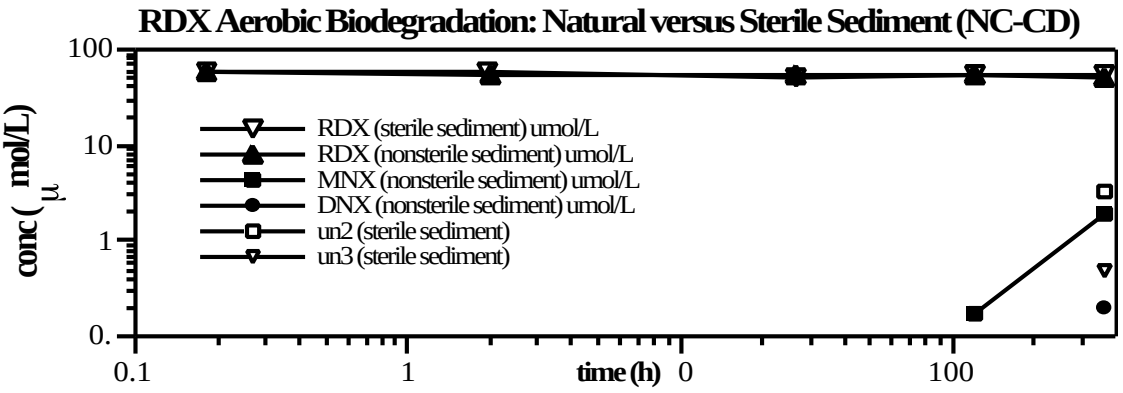
RDX Aerobic Biodegradation: Natural versus Sterile Sediment (NC-CD)
conc (μmol/L)
time (h)
RDX (sterile sediment) umol/L
RDX (nonsterile sediment) umol/L
MNX (nonsterile sediment) umol/L
DNX (nonsterile sediment) umol/L
un2 (sterile sediment)
un3 (sterile sediment)

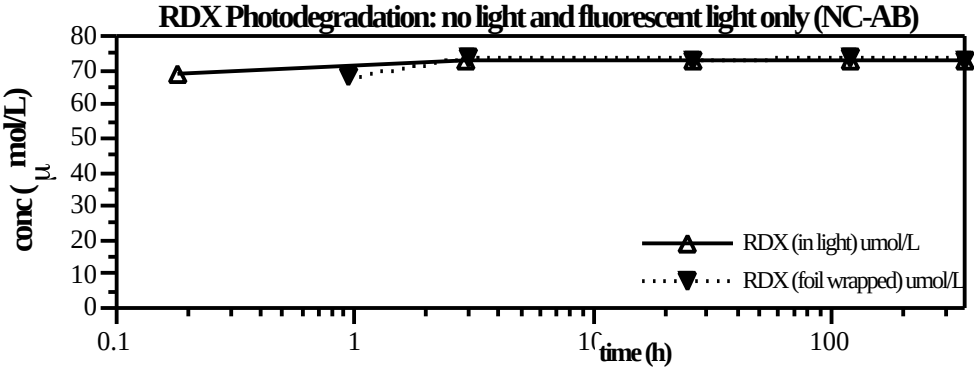
RDX Photodegradation: no light and fluorescent light only (NC-AB)
conc (μmol/L)
time (h)
RDX (in light) umol/L
RDX (foil wrapped) umol/L

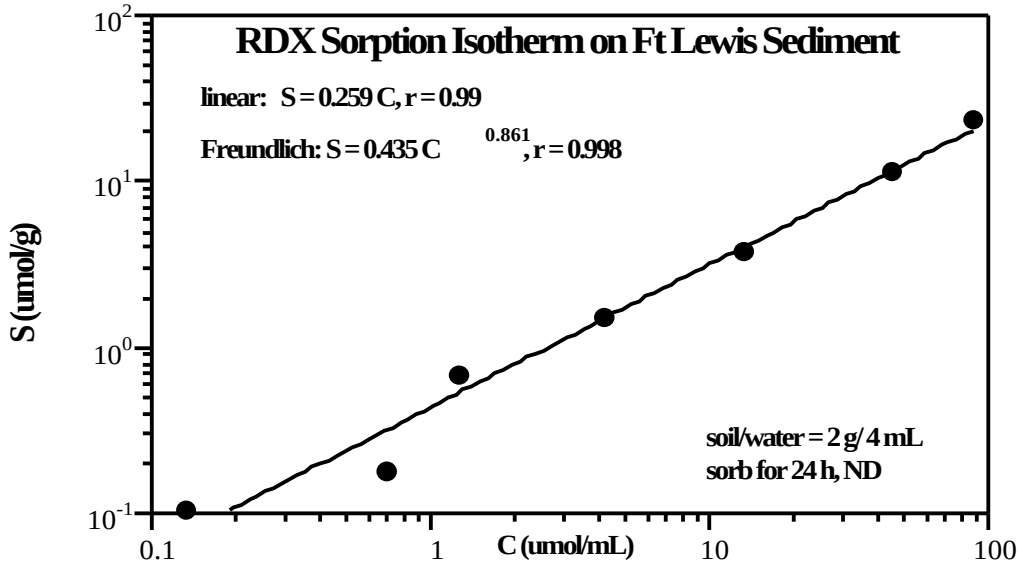
RDX Sorption Isotherm on Ft Lewis Sediment
linear: S = 0.259 C, r = 0.99
Freundlich: S = 0.435 C 0.861, r = 0.998
S (umol/g)
C (umol/mL)
soil/water = 2 g/ 4 mL
sorb for 24 h, ND

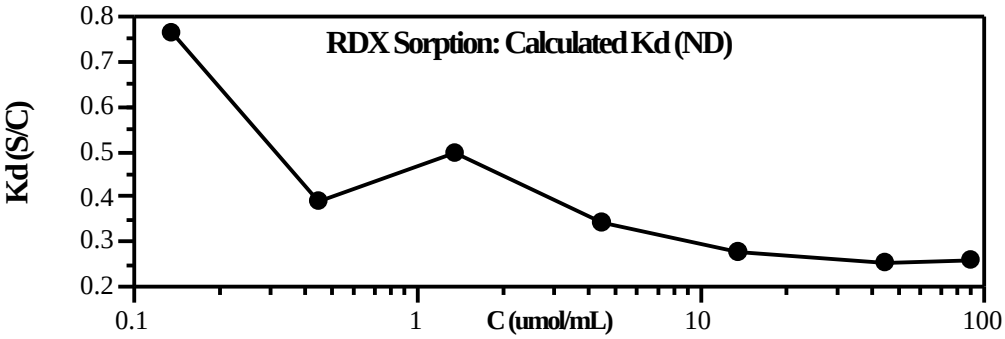
RDX Sorption: Calculated Kd (ND)
Kd (S/C)
0.8
0.7
0.6
0.5
0.4
0.3
0.2
0.1
1
10
100
C (umol/mL)

Appendix E

RDX Column Experiments

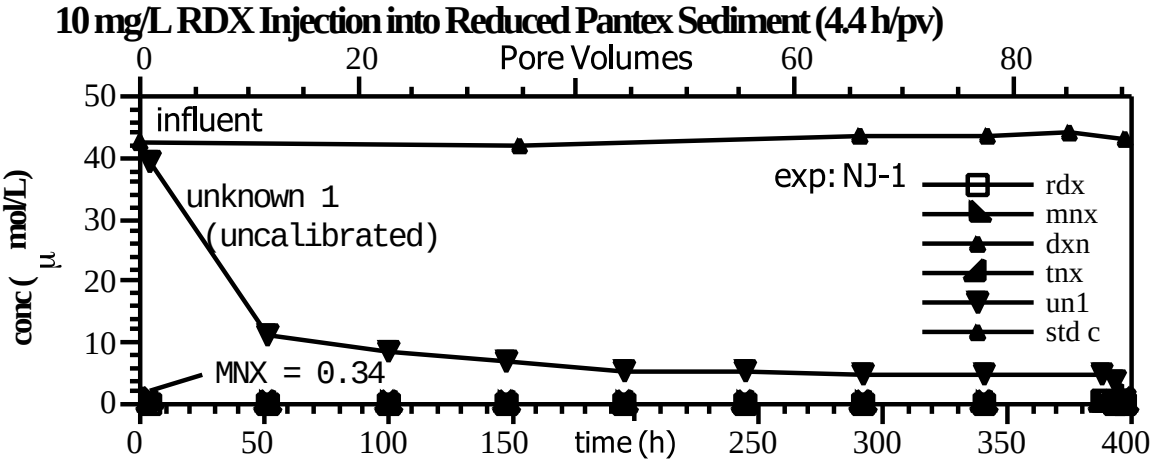
10 mg/L RDX Injection into Reduced Pantex Sediment (4.4 h/pv)
Pore Volumes
influent
unknown 1
(uncalibrated)
MNX = 0.34
exp: NJ-1
rdx
mnx
dxn
tnx
un1
std c
conc (μ mol/L)
time (h)

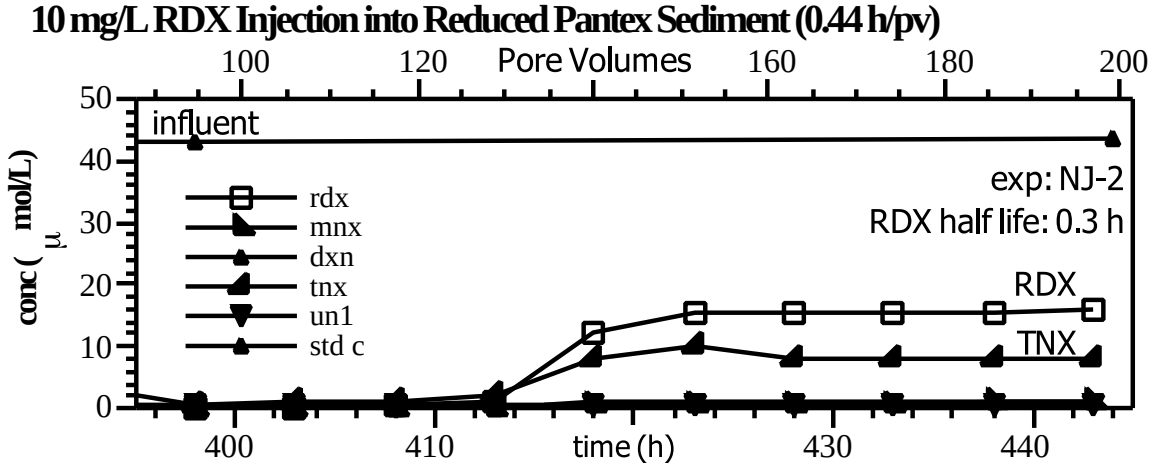
10 mg/L RDX Injection into Reduced Pantex Sediment (0.44 h/pv)
Pore Volumes
influent
exp: NJ-2
RDX half life: 0.3 h
RDX
TNX
rdx
mnx
dxn
tnx
un1
std c
conc (μ mol/L)
time (h)

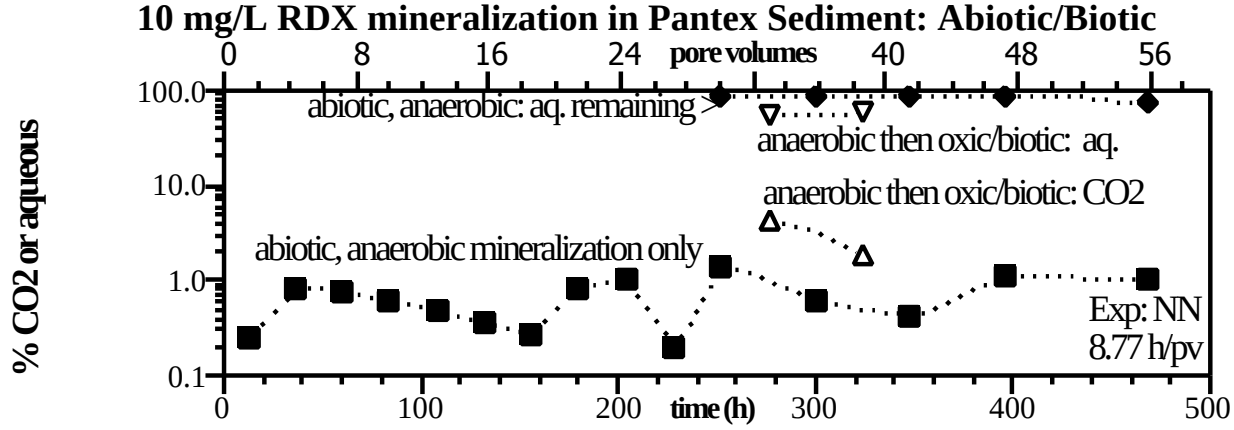
10 mg/L RDX mineralization in Pantex Sediment: Abiotic/Biotic
pore volumes
abiotic, anaerobic: aq. remaining
anaerobic then oxic/biotic: aq.
anaerobic then oxic/biotic: CO2
abiotic, anaerobic mineralization only
Exp: NN
8.77 h/pv
% CO2 or aqueous
time (h)

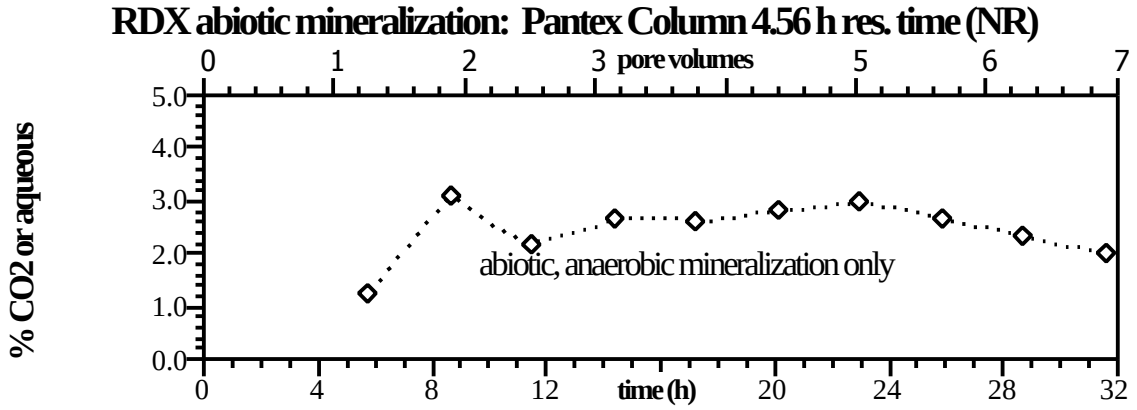
RDX abiotic mineralization: Pantex Column 4.56 h res. time (NR)
pore volumes
% CO2 or aqueous
abiotic, anaerobic mineralization only
time (h)

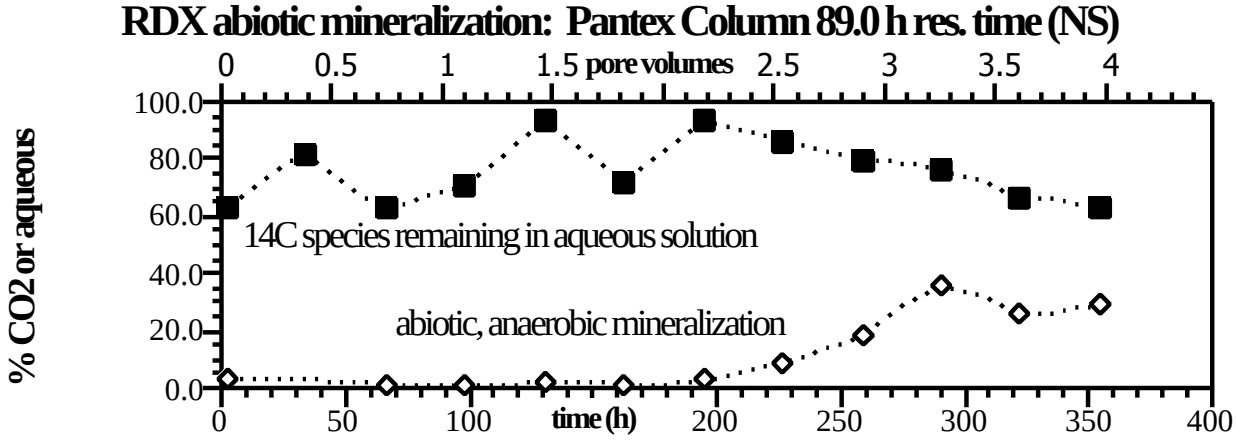
RDX abiotic mineralization: Pantex Column 89.0 h res. time (NS)
pore volumes
% CO2 or aqueous
14C species remaining in aqueous solution
abiotic, anaerobic mineralization
time (h)

Appendix F

Modeling Abiotic RDX Degradation

Model 1: RDX Reduction by Reduced Sediments: Rate Simulations

Reactions as originally written:

1 RDX + 2 Fe2+ <==> MNX + 2Fe3+ + 2OH-
a + 2r <==> b + 2s + 2w with kf1, kb1

2 MNX 2 Fe2+ <==> DNX + 2Fe3+ + 2OH-
b + 2r <==> c + 2s + 2w with kf2, kb2

3 DNX 2 Fe2+ <==> TNX + 2Fe3+ + 2OH-
c + 2r <==> d + 2s + 2w with kf3, kb3

4 TNX 4 Fe2+ <==> UN1 + 4Fe3+ + 2OH-
d + 4r <==> e + 4s + 4w with kf4, kb4

unknown 1 is unidentified, but given little retention on the HPLC column, a guess is that it is a noncyclic such as #8 (McCormick et al ., 1981): N-hydroxymethylmethylenedinitramine (still aqueous)

5 UN1 14 Fe2+ <==> CH3NHNHCH3 + MeOH + HCHO + 14 Fe3+ + 14 OH-
e + 14r <==> f + 14s + 14w with kf53, kb5

for simplicity, compound "f" is the final product, roughly 1,2-dimethylhydrazine

Jim Szecsody
6-27-2001

Species Names:
RDX = A = U0
MNX= B = U1
DXN = C = U2
TNX = D = U3
UN1 = E = U4
hydra = F = U5
Fe2+ = R = U6
Fe3+ = S = U7
OH- =W = U8

If an irreversible (forward or backward) reaction is desired, then make the other rate = 0.0

Note: Input parameters are all rates - if the Kd and one rate is known, calculate the other rate from the Law of Microscopic Reversibility (Kd = kf/kb). Kd is calculated below for convenience, but is not used in calculations!

Consistent units must be used for solution and sorbed species; (umol/cm3), sorbed species*soil/water = umol/g.

All rate parameters are in the same units (1/hr for example), then time steps are in the same units (hours).

Parameters to modify:

$kf1 := 1.50 \cdot 10^{5}$ $kb1 := 0.0$
$kf2 := 2.00 \cdot 10^{6}$ $kb2 := 0.0$
$kf3 := 2.00 \cdot 10^{6}$ $kb3 := 0.0$
$kf4 := 3.50 \cdot 10^{9}$ $kb4 := 0.0$
$kf5 := 1.00 \cdot 10^{30}$ $kb5 := 0.0$

time steps:

$startt := 0.001$
$endt := 10.0$
$n := 2000$

grams sed: mL H2O

$sed := 22.1$
$wat := 130$

this system: 22.1 g sed + 130 ml 0.0796 mol/L di soln

initial estimate of iron in umol/g (convert to mol/L)

mol Fe/L = X umol/g * mol/10^6 umol * 22.1 g / 0.13 L

q = mol Fe/L to umol/g conversion, = 10^6 * Y liters / Z g sediment

$q := 1000 \cdot \frac{wat}{sed}$

$q = 5.882 \cdot 10^{3}$

Partial differential equations for each chemical component:

$da(a, b, c, d, e, f, r, s, w) := -kf1 \cdot a \cdot r^2 + kb1 \cdot b \cdot s^2 \cdot w^2$

$db(a, b, c, d, e, f, r, s, w) := kf1 \cdot a \cdot r^2 - kb1 \cdot b \cdot s^2 \cdot w^2 - kf2 \cdot b \cdot r^2 + kb2 \cdot c \cdot s^2 \cdot w^2$

$dc(a, b, c, d, e, f, r, s, w) := kf2 \cdot b \cdot r^2 - kb2 \cdot c \cdot s^2 \cdot w^2 - kf3 \cdot c \cdot r^2 + kb3 \cdot d \cdot s^2 \cdot w^2$

$dd(a, b, c, d, e, f, r, s, w) := kf3 \cdot c \cdot r^2 - kb3 \cdot d \cdot s^2 \cdot w^2 - kf4 \cdot d \cdot r^4 + kb4 \cdot e \cdot s^4 \cdot w^4$

$de(a, b, c, d, e, f, r, s, w) := kf4 \cdot d \cdot r^4 - kb4 \cdot e \cdot s^4 \cdot w^4 - kf5 \cdot e \cdot r^{14} + kb5 \cdot f \cdot s^{14} \cdot w^{14}$

$df(a, b, c, d, e, f, r, s, w) := 14 \cdot kf5 \cdot e \cdot r^{14} - 14 \cdot kb5 \cdot f \cdot s^{14} \cdot w^{14}$

$zef(a, b, c, d, e, f, r, s, w) := -4 \cdot kf4 \cdot d \cdot r^4 + 4 \cdot kb4 \cdot e \cdot s^4 \cdot w^4 - 14 \cdot kf5 \cdot e \cdot r^{14} + 14 \cdot kb5 \cdot f \cdot s^{14} \cdot w^{14}$

$dr(a, b, c, d, e, f, r, s, w) := -2 \cdot kf1 \cdot a \cdot r^2 + 2 \cdot kb1 \cdot b \cdot s^2 \cdot w^2 - 2 \cdot kf2 \cdot b \cdot r^2 + 2 \cdot kb2 \cdot c \cdot s^2 \cdot w^2 - 2 \cdot kf3 \cdot c \cdot r^2 + 2 \cdot kb3 \cdot d \cdot s^2 \cdot w^2 + zef(a, b, c, d, e, f, r, s, w)$

$ds(a, b, c, d, e, f, r, s, w) := \left(2 \cdot kf1 \cdot a \cdot r^2 - 2 \cdot kb1 \cdot b \cdot s^2 \cdot w^2 + 2 \cdot kf2 \cdot b \cdot r^2 - 2 \cdot kb2 \cdot c \cdot s^2 \cdot w^2 - 2 \cdot kf3 \cdot c \cdot r^2\right) + 2 \cdot kb3 \cdot d \cdot s^2 \cdot w^2 - zef(a, b, c, d, e, f, r, s, w)$

$dw(a, b, c, d, e, f, r, s, w) := \left(2 \cdot kf1 \cdot a \cdot r^2 - 2 \cdot kb1 \cdot b \cdot s^2 \cdot w^2 + 2 \cdot kf2 \cdot b \cdot r^2 - 2 \cdot kb2 \cdot c \cdot s^2 \cdot w^2 - 2 \cdot kf3 \cdot c \cdot r^2\right) + 2 \cdot kb3 \cdot d \cdot s^2 \cdot w^2 - zef(a, b, c, d, e, f, r, s, w)$

Initial conditions (note: write in mol/L, then convert back to mol or mol/g:

Derivative vector:

Model 2: RDX Degradation by Reduced Sediment - Variable Order Reactions

Reactions as originally written: ****all reactions with variable order on first term****

1 RDX + 2 Fe2+ <==> MNX + 2Fe3+ + 2OH-
(n1) a + 2r <==> b + 2s + 2w with kf1, kb1

2 MNX + 2 Fe2+ <==> DNX + 2Fe3+ + 2OH-
(n2)b + 2r <==> c + 2s + 2w with kf2, kb2

3 DNX + 2 Fe2+ <==> TNX + 2Fe3+ + 2OH-
(n3) c + 2r <==> d + 2s + 2w with kf3, kb3

4 TNX + 4 Fe2+ <==> UN1 + 4Fe3+ + 2OH-
(n4) d + 4r <==> e + 4s + 4w with kf4, kb4

unknown 1 is unidentified, but given little retention on the HPLC column, a guess is that it is a noncyclic such as #8 (McCormick et al ., 1981): N-hydroxymethylmethylenedinitramine (still aqueous)

5 UN1 + 14 Fe2+ <==> CH3NHNHCH3 + MeOH + HCHO + 14 Fe3+ + 14 OH-
(n5) e + 14r <==> f + 14s + 14w with kf53, kb5

for simplicity, compound "f" is the final product, roughly 1,2-dimethylhydrazine

Jim Szecsody
7-16-2001

Species Names:
RDX = A = U0
MNX= B = U1
DXN = C = U2
TNX = D = U3
UN1 = E = U4
hydra = F = U5
Fe2+ = R = U6
Fe3+ = S = U7
OH- =W = U8

If an irreversible (forward or backward) reaction is desired, then make the other rate = 0.0
Note: Input parameters are all rates - if the Kd and one rate is known, calculate the other rate from the Law of Microscopic Reversibility (Kd = kf/kb). Kd is calculated below for convenience, but is not used in calculations!
Consistent units must be used for solution and sorbed species; (umol/cm3), sorbed species*soil/water = umol/g.
All rate parameters are in the same units (1/hr for example), then time steps are in the same units (hours).

Parameters to modify:

$kf1 := 2\cdot 10^{4}$ $kb1 := 0.0$ $n1 := 1.0$
$kf2 := 2.5\cdot 10^{5}$ $kb2 := 0.0$ $n2 := 1.0$
$kf3 := 1.8\cdot 10^{5}$ $kb3 := 0.0$ $n3 := 1.0$
$kf4 := 5\cdot 10^{8}$ $kb4 := 0.0$ $n4 := 1.0$
$kf5 := 0.0$ $kb5 := 0.0$ $n5 := 1.0$

time steps: $startt := 0.001$ $endt := 10.0$ $n := 2000$

grams sed: $sed := 22.1$
mL H2O $wat := 130$

Partial differential equations for each chemical component:

this system: 22.1 g sed + 130 ml 0.0796 mol/L di soln

$da(a,b,c,d,e,f,r,s,w) := -kf1\cdot n1\cdot a^{n1}\cdot r^{2} + kb1\cdot b\cdot s^{2}\cdot w^{2}$

$db(a,b,c,d,e,f,r,s,w) := kf1\cdot n1\cdot a^{n1}\cdot r^{2} - kb1\cdot b\cdot s^{2}\cdot w^{2} - kf2\cdot n2\cdot b^{n2}\cdot r^{2} + kb2\cdot c\cdot s^{2}\cdot w^{2}$

initial estimate of iron in umol/g (convert to mol/L)

$dc(a,b,c,d,e,f,r,s,w) := kf2\cdot n2\cdot b^{n2}\cdot r^{2} - kb2\cdot c\cdot s^{2}\cdot w^{2} - kf3\cdot n3\cdot c^{n3}\cdot r^{2} + kb3\cdot d\cdot s^{2}\cdot w^{2}$

mol Fe/L = X umol/g * mol/10^6 umol * 22.1 g / 0.13 L

$dd(a,b,c,d,e,f,r,s,w) := kf3\cdot n3\cdot c^{n3}\cdot r^{2} - kb3\cdot d\cdot s^{2}\cdot w^{2} - kf4\cdot n4\cdot d^{n4}\cdot r^{4} + kb4\cdot e\cdot s^{4}\cdot w^{4}$

$de(a,b,c,d,e,f,r,s,w) := kf4\cdot n4\cdot d^{n4}\cdot r^{4} - kb4\cdot e\cdot s^{4}\cdot w^{4} - kf5\cdot n5\cdot e^{n5}\cdot r^{14} + kb5\cdot f\cdot s^{14}\cdot w^{14}$

q = mol Fe/L to umol/g conversion, = 10^6 * Y liters / Z g sediment

$q := 1000\cdot\frac{wat}{sed}$

$df(a,b,c,d,e,f,r,s,w) := 1\cdot kf5\cdot n5\cdot e^{n5}\cdot r^{14} - 1\cdot kb5\cdot f\cdot s^{14}\cdot w^{14}$

$q = 5.882\cdot 10^{3}$

$zef(a,b,c,d,e,f,r,s,w) := -4\cdot kf4\cdot d^{n4}\cdot r^{4} + 4\cdot kb4\cdot e\cdot s^{4}\cdot w^{4} - 14\cdot kf5\cdot e^{n5}\cdot r^{14} + 14\cdot kb5\cdot f\cdot s^{14}\cdot w^{14}$

$dr(a,b,c,d,e,f,r,s,w) := -2\cdot kf1\cdot a^{n1}\cdot r^{2} + 2\cdot kb1\cdot b\cdot s^{2}\cdot w^{2} - 2\cdot kf2\cdot b^{n2}\cdot r^{2} + 2\cdot kb2\cdot c\cdot s^{2}\cdot w^{2} - 2\cdot kf3\cdot c^{n3}\cdot r^{2} + 2\cdot kb3\cdot d\cdot s^{2}\cdot w^{2} + zef(a,b,c,d,e,f,r,s,w)$

$ds(a,b,c,d,e,f,r,s,w) := 2\cdot kf1\cdot a^{n2}\cdot r^{2} - 2\cdot kb1\cdot b\cdot s^{2}\cdot w^{2} + 2\cdot kf2\cdot b^{n2}\cdot r^{2} - 2\cdot kb2\cdot c\cdot s^{2}\cdot w^{2} - 2\cdot kf3\cdot c^{n3}\cdot r^{2} + 2\cdot kb3\cdot d\cdot s^{2}\cdot w^{2} - zef(a,b,c,d,e,f,r,s,w)$

$dw(a,b,c,d,e,f,r,s,w) := 2\cdot kf1\cdot a^{n1}\cdot r^{2} - 2\cdot kb1\cdot b\cdot s^{2}\cdot w^{2} + 2\cdot kf2\cdot b^{n2}\cdot r^{2} - 2\cdot kb2\cdot c\cdot s^{2}\cdot w^{2} - 2\cdot kf3\cdot c^{n3}\cdot r^{2} + 2\cdot kb3\cdot d\cdot s^{2}\cdot w^{2} - zef(a,b,c,d,e,f,r,s,w)$

Model 3: RDX Reduction by Reduced Sediments and Adsorption: Rate Simulations

Jim Szecsody
8-20-2001

Reactions as originally written:

1 RDX + 2 Fe2+ <==> MNX + 2Fe3+ + 2OH-
a + 2r <==> b + 2s + 2w with kf1, kb1

2 MNX 2 Fe2+ <==> DNX + 2Fe3+ + 2OH-
b + 2r <==> c + 2s + 2w with kf2, kb2

3 DNX 2 Fe2+ <==> TNX + 2Fe3+ + 2OH-
c + 2r <==> d + 2s + 2w with kf3, kb3

4 TNX 4 Fe2+ <==> UN1 + 4Fe3+ + 2OH-
d + 4r <==> e + 4s + 4w with kf4, kb4

unknown 1 is unidentified, but given little retention on the HPLC column, a guess is that it is a noncyclic such as #8 (McCormick et al ., 1981): N-hydroxymethylmethylenedinitramine (still aqueous)

5 UN1 14 Fe2+ <==> CH3NHNHCH3 + MeOH + HCHO + 14 Fe3+ + 14 OH-
e + 14r <==> f + 14s + 14w with kf53, kb5

for simplicity, compound "f" is the final product, roughly 1,2-dimethylhydrazine

6 RDX <==> S-RDX

7 MNX <==> S-MNX

8 DNX <==> S-DNX

9 TNX <==> S-TNX

Species Names:
RDX = A = U0
MNX= B = U1
DXN = C = U2
TNX = D = U3
UN1 = E = U4
hydra = F = U5
Fe2+ = R = U6
Fe3+ = S = U7
OH- =W = U8
S-RDX=SA=U9
S-MNX=SB=U10
S-DNX=SC=U11
S-TNX=SD=U12

Parameters to modify:

$kf1 := 6.5 \cdot 10^{6}$ $kb1 := 0.0$
$kf2 := 8.00 \cdot 10^{6}$ $kb2 := 0.0$
$kf3 := 2.00 \cdot 10^{6}$ $kb3 := 0.0$
$kf4 := 3.50 \cdot 10^{0}$ $kb4 := 0.0$
$kf5 := 0$ $kb5 := 0.0$
$kf6 := 1$ $kb6 := 1.0$
$kf7 := 1$ $kb7 := 1.0$
$kf8 := 1$ $kb8 := 1.0$
$kf9 := 0.0$ $kb9 := 1.0$

time steps: $startt := 0.001$ $endt := 10.$ $n := 2000$

grams sed: $sed := 22.1$
mL H2O: $wat := 130$

this system: 22.1 g sed + 130 ml 0.0796 mol/L di soln

initial estimate of iron in umol/g (convert to mol/L)

mol Fe/L = X umol/g * mol/10^6 umol * 22.1 g / 0.13 L

q = mol Fe/L to umol/g conversion,
= 10^6 * Y liters / Z g sediment

$q := 1000 \cdot \frac{wat}{sed}$

$q = 5.882 \cdot 10^{3}$

Partial differential equations for each chemical component:

$$da(a,b,c,d,e,f,r,s,w,sa,sb,sc,sd) := -kf1 \cdot a \cdot r^2 + kb1 \cdot b \cdot s^2 \cdot w^2 - kf6 \cdot a + kb6 \cdot a$$

$$db(a,b,c,d,e,f,r,s,w,sa,sb,sc,sd) := kf1 \cdot a \cdot r^2 - kb1 \cdot b \cdot s^2 \cdot w^2 - kf2 \cdot b \cdot r^2 + kb2 \cdot c \cdot s^2 \cdot w^2 - kf7 \cdot b + kb7 \cdot b$$

$$dc(a,b,c,d,e,f,r,s,w,sa,sb,sc,sd) := kf2 \cdot b \cdot r^2 - kb2 \cdot c \cdot s^2 \cdot w^2 - kf3 \cdot c \cdot r^2 + kb3 \cdot d \cdot s^2 \cdot w^2 - kf8 \cdot c + kb8 \cdot c$$

$$dd(a,b,c,d,e,f,r,s,w,sa,sb,sc,sd) := kf3 \cdot c \cdot r^2 - kb3 \cdot d \cdot s^2 \cdot w^2 - kf4 \cdot d \cdot r^4 + kb4 \cdot e \cdot s^4 \cdot w^4 - kf9 \cdot d + kb9 \cdot d$$

$$de(a,b,c,d,e,f,r,s,w,sa,sb,sc,sd) := kf4 \cdot d \cdot r^4 - kb4 \cdot e \cdot s^4 \cdot w^4 - kf5 \cdot e \cdot r^{14} + kb5 \cdot f \cdot s^{14} \cdot w^{14} - (kf7 \cdot b + kb7 \cdot b)$$

$$df(a,b,c,d,e,f,r,s,w,sa,sb,sc,sd) := 14 \cdot kf5 \cdot e \cdot r^{14} - 14 \cdot kb5 \cdot f \cdot s^{14} \cdot w^{14}$$

$$dr(a,b,c,d,e,f,r,s,w,sa,sb,sc,sd) := -2 \cdot kf1 \cdot a \cdot r^2 + 2 \cdot kb1 \cdot b \cdot s^2 \cdot w^2 - 2 \cdot kf2 \cdot b \cdot r^2 + 2 \cdot kb2 \cdot c \cdot s^2 \cdot w^2 - 2 \cdot kf3 \cdot c \cdot r^2 + 2 \cdot kb3 \cdot d \cdot s^2 \cdot w^2 + -4 \cdot kf4 \cdot d \cdot r^4 + 4 \cdot kb4 \cdot e \cdot s^4 \cdot w^4 - 14 \cdot kf5 \cdot e \cdot r^{14} + 14 \cdot kb5 \cdot f \cdot s^{14} \cdot w^{14}$$

$$ds(a,b,c,d,e,f,r,s,w,sa,sb,sc,sd) := (2 \cdot kf1 \cdot a \cdot r^2 - 2 \cdot kb1 \cdot b \cdot s^2 \cdot w^2 + 2 \cdot kf2 \cdot b \cdot r^2 - 2 \cdot kb2 \cdot c \cdot s^2 \cdot w^2 - 2 \cdot kf3 \cdot c \cdot r^2) + 2 \cdot kb3 \cdot d \cdot s^2 \cdot w^2 - (-4 \cdot kf4 \cdot d \cdot r^4 + 4 \cdot kb4 \cdot e \cdot s^4 \cdot w^4 - 14 \cdot kf5 \cdot e \cdot r^{14} + 14 \cdot kb5 \cdot f \cdot s^{14} \cdot w^{14})$$

$$dw(a,b,c,d,e,f,r,s,w,sa,sb,sc,sd) := (2 \cdot kf1 \cdot a \cdot r^2 - 2 \cdot kb1 \cdot b \cdot s^2 \cdot w^2 + 2 \cdot kf2 \cdot b \cdot r^2 - 2 \cdot kb2 \cdot c \cdot s^2 \cdot w^2 - 2 \cdot kf3 \cdot c \cdot r^2) + 2 \cdot kb3 \cdot d \cdot s^2 \cdot w^2 - (-4 \cdot kf4 \cdot d \cdot r^4 + 4 \cdot kb4 \cdot e \cdot s^4 \cdot w^4 - 14 \cdot kf5 \cdot e \cdot r^{14} + 14 \cdot kb5 \cdot f \cdot s^{14} \cdot w^{14})$$

$$dsa(a,b,c,d,e,f,r,s,w,sa,sb,sc,sd) := kf6 \cdot a - kb6 \cdot a$$

$$dsb(a,b,c,d,e,f,r,s,w,sa,sb,sc,sd) := kf7 \cdot b - kb7 \cdot b$$

$$dsc(a,b,c,d,e,f,r,s,w,sa,sb,sc,sd) := kf8 \cdot c - kb8 \cdot c$$

$$dsd(a,b,c,d,e,f,r,s,w,sa,sb,sc,sd) := kf9 \cdot d - kb9 \cdot d$$

Appendix G

Simulations of Batch RDX Degradation

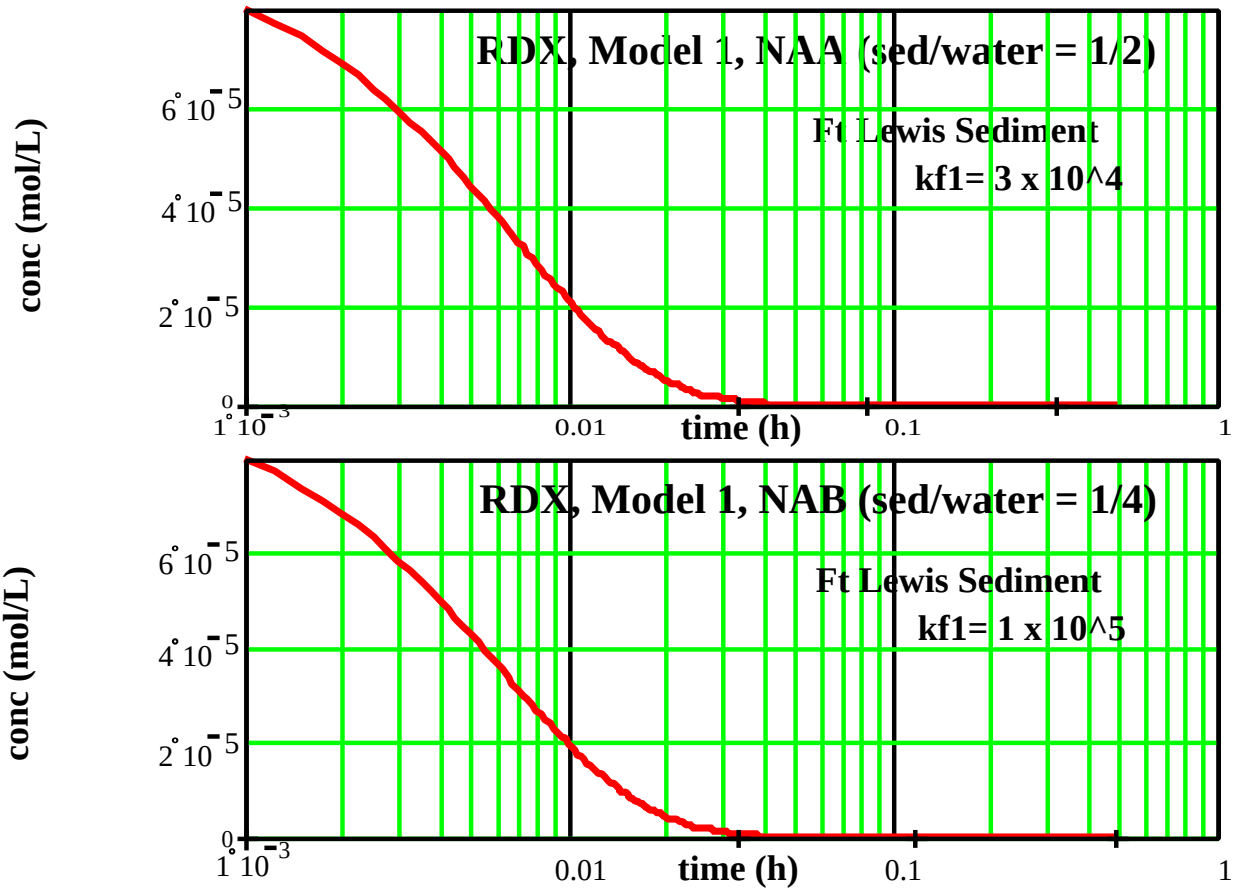
RDX, Model 1, NAA (sed/water = 1/2)
Ft Lewis Sediment
kf1= 3 x 10^4
conc (mol/L)
6·10^-5
4·10^-5
2·10^-5
0
1·10^-3
0.01
0.1
1
time (h)
RDX, Model 1, NAB (sed/water = 1/4)
Ft Lewis Sediment
kf1= 1 x 10^5
conc (mol/L)
6·10^-5
4·10^-5
2·10^-5
0
1·10^-3
0.01
0.1
1
time (h)

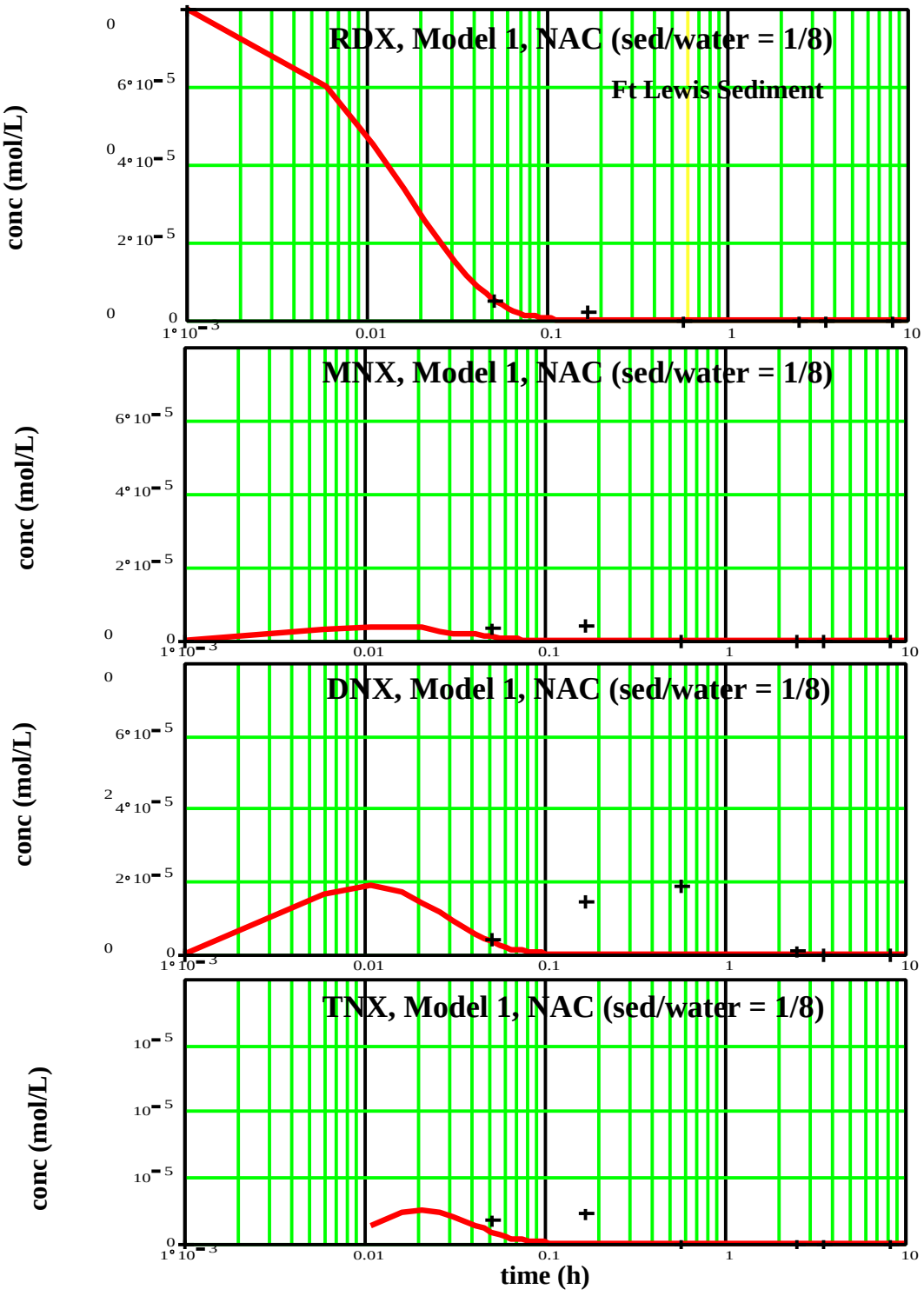
RDX, Model 1, NAC (sed/water = 1/8)
Ft Lewis Sediment
MNX, Model 1, NAC (sed/water = 1/8)
DNX, Model 1, NAC (sed/water = 1/8)
TNX, Model 1, NAC (sed/water = 1/8)
conc (mol/L)
time (h)
0.01
0.1
1
10

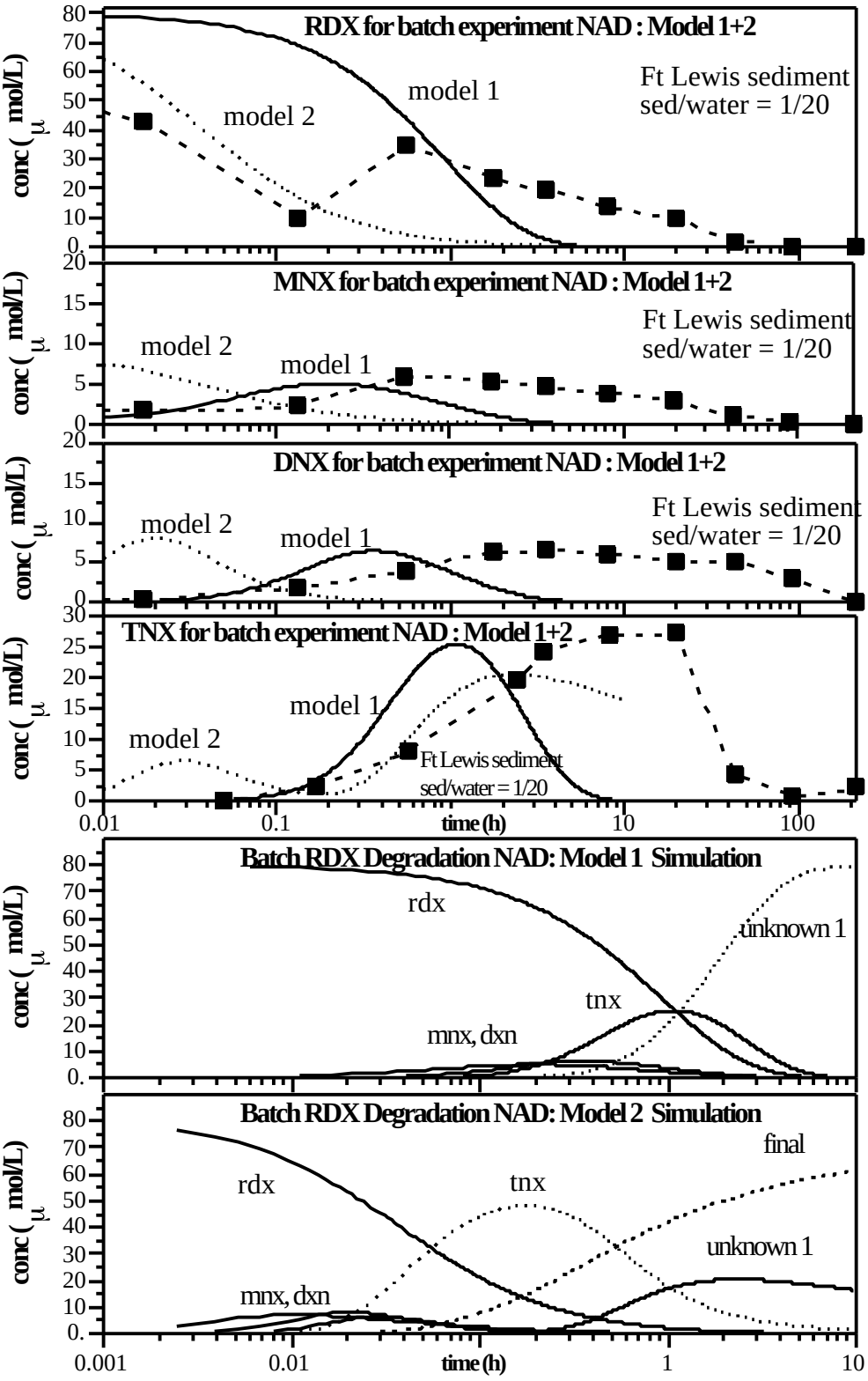
RDX for batch experiment NAD : Model 1+2
model 1
model 2
Ft Lewis sediment
sed/water = 1/20
conc (µ mol/L)
MNX for batch experiment NAD : Model 1+2
model 2
model 1
Ft Lewis sediment
sed/water = 1/20
DNX for batch experiment NAD : Model 1+2
model 2
model 1
Ft Lewis sediment
sed/water = 1/20
TNX for batch experiment NAD : Model 1+2
model 1
model 2
Ft Lewis sediment
sed/water = 1/20
time (h)
Batch RDX Degradation NAD: Model 1 Simulation
rdx
unknown 1
tnx
mnx, dxn
Batch RDX Degradation NAD: Model 2 Simulation
final
rdx
tnx
unknown 1
mnx, dxn
time (h)

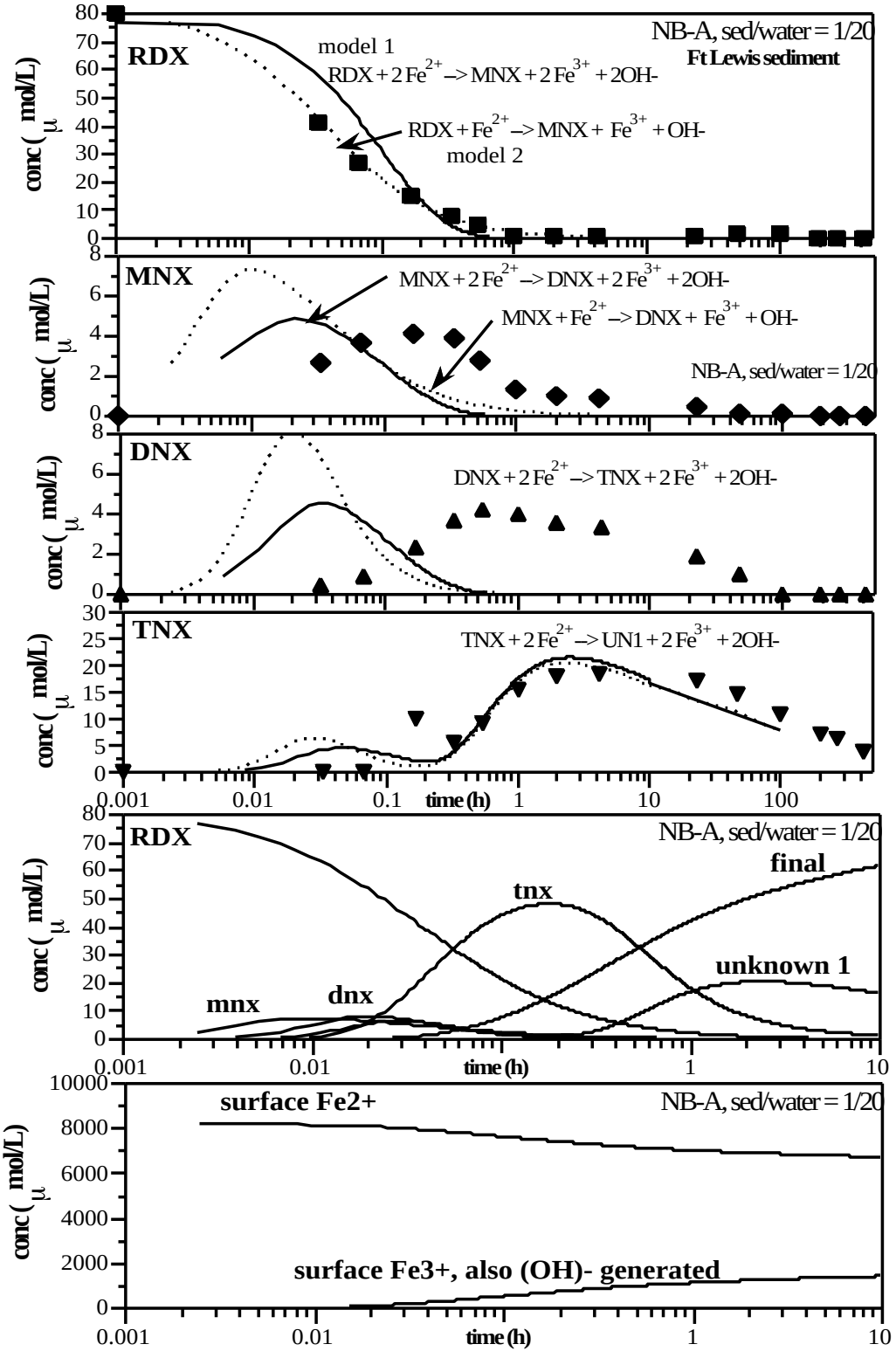
RDX
model 1
RDX + 2 Fe2+ –> MNX + 2 Fe3+ + 2OH-
RDX + Fe2+ –> MNX + Fe3+ + OH-
model 2
NB-A, sed/water = 1/20
Ft Lewis sediment
conc (μ mol/L)
MNX
MNX + 2 Fe2+ –> DNX + 2 Fe3+ + 2OH-
MNX + Fe2+ –> DNX + Fe3+ + OH-
NB-A, sed/water = 1/20
DNX
DNX + 2 Fe2+ –> TNX + 2 Fe3+ + 2OH-
TNX
TNX + 2 Fe2+ –> UN1 + 2 Fe3+ + 2OH-
time (h)
RDX
NB-A, sed/water = 1/20
final
tnx
unknown 1
mnx
dnx
surface Fe2+
NB-A, sed/water = 1/20
surface Fe3+, also (OH)- generated

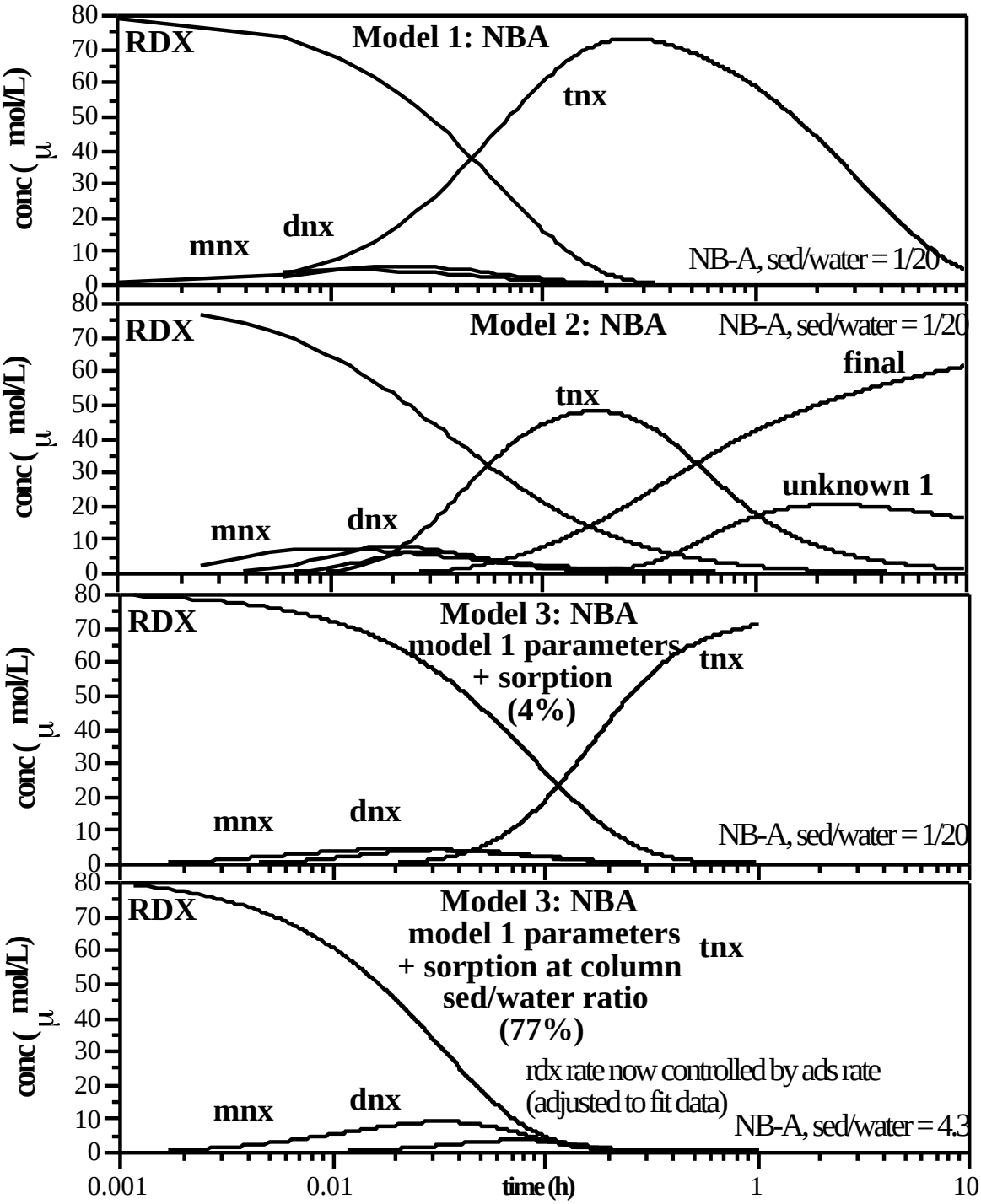
Model 1: NBA
RDX
tnx
dnx
mnx
NB-A, sed/water = 1/20
Model 2: NBA
NB-A, sed/water = 1/20
final
unknown 1
Model 3: NBA
model 1 parameters
+ sorption
(4%)
Model 3: NBA
model 1 parameters
+ sorption at column
sed/water ratio
(77%)
rdx rate now controlled by ads rate
(adjusted to fit data)
NB-A, sed/water = 4.3
conc (μ mol/L)
time (h)
0.001
0.01
1
10

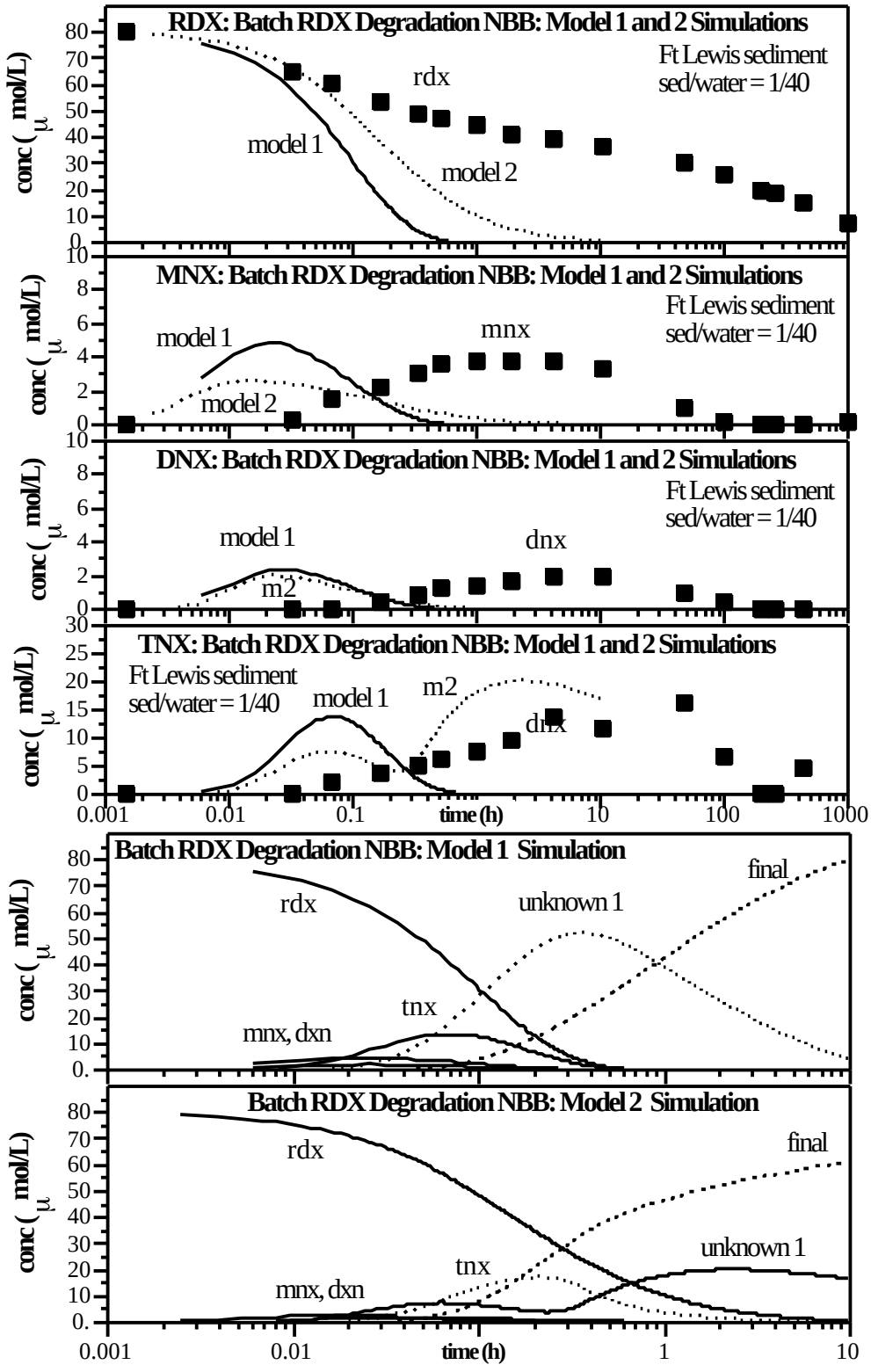
RDX: Batch RDX Degradation NBB: Model 1 and 2 Simulations
Ft Lewis sediment
sed/water = 1/40
rdx
model 1
model 2
conc (μ mol/L)
MNX: Batch RDX Degradation NBB: Model 1 and 2 Simulations
Ft Lewis sediment
sed/water = 1/40
model 1
mnx
model 2
conc (μ mol/L)
DNX: Batch RDX Degradation NBB: Model 1 and 2 Simulations
Ft Lewis sediment
sed/water = 1/40
model 1
dnx
m2
conc (μ mol/L)
TNX: Batch RDX Degradation NBB: Model 1 and 2 Simulations
Ft Lewis sediment
sed/water = 1/40
model 1
m2
dnx
conc (μ mol/L)
0.001
0.01
0.1
time (h)
10
100
1000
Batch RDX Degradation NBB: Model 1 Simulation
rdx
unknown 1
final
tnx
mnx, dxn
conc (μ mol/L)
Batch RDX Degradation NBB: Model 2 Simulation
rdx
final
unknown 1
tnx
mnx, dxn
conc (μ mol/L)
0.001
0.01
time (h)
1
10

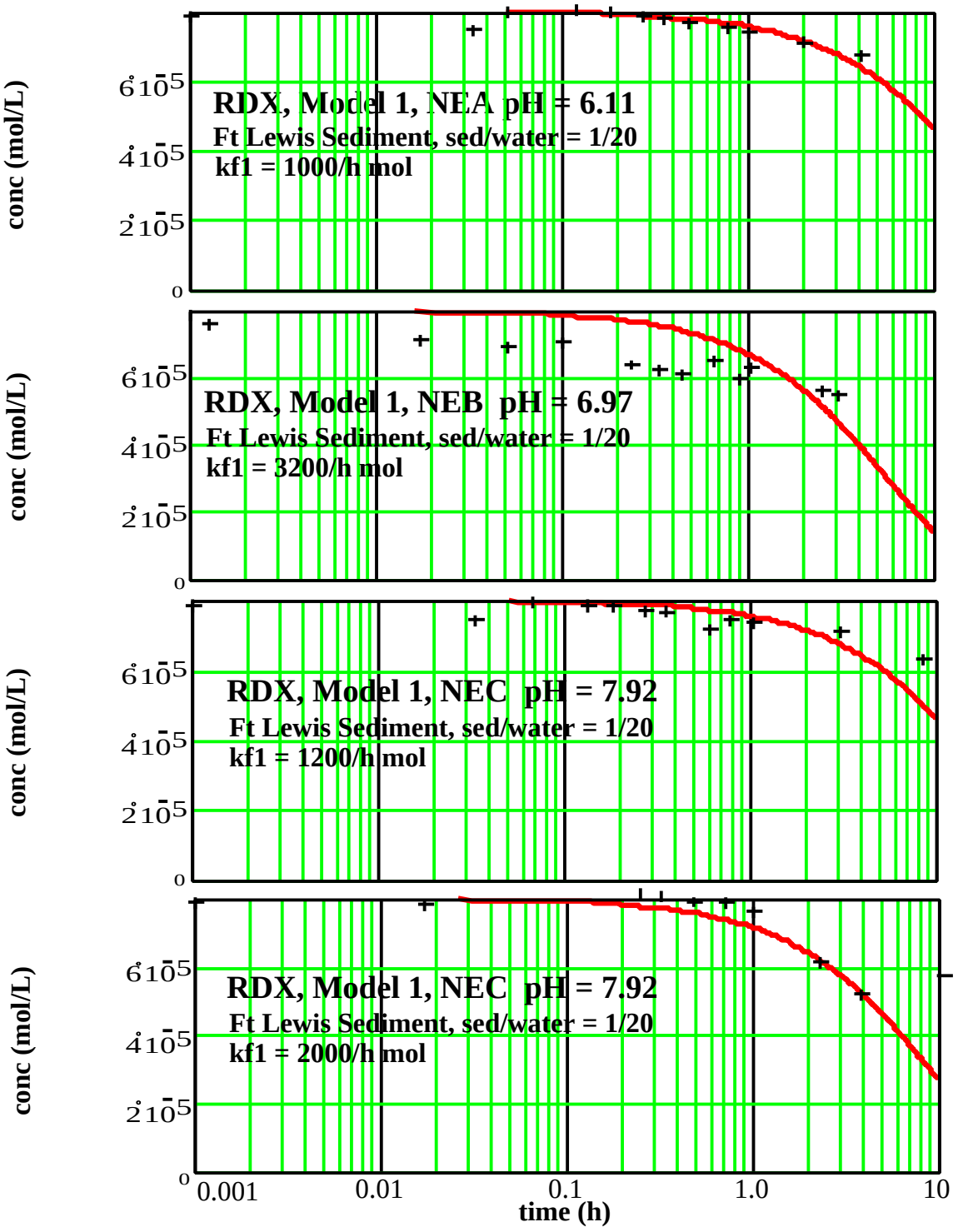
RDX, Model 1, NEA pH = 6.11
Ft Lewis Sediment, sed/water = 1/20
kf1 = 1000/h mol
RDX, Model 1, NEB pH = 6.97
Ft Lewis Sediment, sed/water = 1/20
kf1 = 3200/h mol
RDX, Model 1, NEC pH = 7.92
Ft Lewis Sediment, sed/water = 1/20
kf1 = 1200/h mol
RDX, Model 1, NEC pH = 7.92
Ft Lewis Sediment, sed/water = 1/20
kf1 = 2000/h mol
conc (mol/L)
6·10^-5
4·10^-5
2·10^-5
0
0.001
0.01
0.1
1.0
10
time (h)

Distribution

No. of Copies

OFFSITE

6 J. Phelan
Sandia National Laboratories
P.O. Box 5800, MS 0779
Albuquerque, NM 87185

ONSITE

24 **Pacific Northwest National Laboratory**

J. E. Amonette	K8-96
J. Bush	K6-96
W. F. Bonner (3)	K9-14
J. S. Fruchter	K6-96
T. J Gilmore	K6-81
S. G. McKinley	P7-07
C. T. Resch	K3-61
J. E. Szecsody (10)	K3-61
V. R. Vermeul	K6-96
M. D. Williams	K9-36
J. M. Zachara	K8-96
Hanford Technical Library (2)	P8-55